Online distributed price-based control of DR resources with competitive guarantees

Siyuan Xu
Liren Yu
Xiaojun Lin
School of Electrical and Computer Engineering
Purdue University, West Lafayette
{xu1082,yu827,linx}@purdue.edu

Jin Dong
Yaosuo Xue
Oak Ridge National Laboratory
{dongj,xuey}@ornl.gov

ABSTRACT

Demand response (DR) of building HVAC load can provide crucial demand-side flexibility for the future smart grid. Compared to direct load control, price-based control can respect the customers' autonomy and privacy. However, it is challenging for price-based control to attain provable performance guarantees under future uncertainty. In this paper, we propose a framework for a utility to perform price-based control of flexible building load within the utility's service area, in order to attain competitive performance guarantees in terms of controlling the system peak demand under future uncertainty. By adopting a two-step approach, our online price-based control solution can attain a provable competitive ratio for all possible realizations within a given uncertainty set. Simulation experiments demonstrate that, with a robustification procedure, our solution can perform well not only for worst-case inputs, but also for average-case inputs.

CCS CONCEPTS

• **Hardware** → **Smart grid**; • **Mathematics of computing** → **Mathematical analysis**.

KEYWORDS

Demand response, competitive online algorithm, price-based control, peak demand.

ACM Reference Format:
Siyuan Xu, Liren Yu, Xiaojun Lin, Jin Dong, and Yaosuo Xue. 2022. Online distributed price-based control of DR resources with competitive guarantees. In *The Thirteenth ACM International Conference on Future Energy Systems (e-Energy '22), June 28-July 1, 2022, Virtual Event, USA.* ACM, New York, NY, USA, 17 pages. https://doi.org/10.1145/3538637.3538836

1 INTRODUCTION

Demand response (DR) is considered crucial for future smart grid [4, 5, 20]. By invoking the flexibility of the demand side, the electricity consumption can be adjusted to offset the variability and uncertainty of renewable generation, which can shave system peak and benefit system reliability. Buildings, in particular their HVAC (heating, ventilation and air-conditioning) systems, both consume a significant amount of electricity [29] and offer significant flexibility [22]. Indeed, HVAC of typical buildings consumes about 25-40% of the building electricity load [3], and buildings consume about 70% of the total electrical consumption in the U.S. [6]. Thus, there are significant interests in demand response for building load [7].

Existing techniques on residential demand response can be classified into two main categories: Direct Load Control (DLC) and price-based control. With DLC, utilities can directly give orders to customers who sign up for the DLC program [9, 27], e.g., shutting down their appliances during high demand period [10]. In return, customers would receive financial compensation for the participation. However, DLC is usually considered too intrusive, especially for buildings who must also maintain their own business interests [16, 32]. Price-based approaches, on the other hand, assume that utility can only send price incentive signals. Customers can decide how they will respond to the incentive signals [15] based on their own preference. This form of control is therefore more favorable when customers wish to retain their autonomy and privacy.

One of the difficulties of price-based control, however, is that it becomes much more difficult for the system controller (i.e., utilities) to attain performance guarantees, especially when there is significant uncertainty in future inputs (e.g., load and renewable generation). We note that there has been a significant body of literature on how to compute the appropriate price signals to achieve system-wide objectives even when the utility does not exactly know the internal parameters of the consumers (see, e.g., [25]). However, most of these studies assume that the future inputs are known [21, 31]. In reality, key inputs, e.g., future renewable generation, have significant uncertainty [33]. One may use Model Predictive Control (MPC) or Receding Horizon Control (RHC) [2, 23] to deal with such uncertainty, i.e., first compute prices based on predicted inputs, then adjust prices as new inputs are revealed. However, such approaches usually cannot provide strong guarantees on how good the performance (e.g., the system peak) remains when the actual inputs substantially deviate from their predicted values. This situation is in sharp contrast to the DLC setting, where competitive online algorithms [34] can be developed to attain a provable competitive ratio for *all* possible future inputs in a given uncertainty set. Thus, it remains an open question how to develop algorithms for distributed price-based control of DR resources to attain competitive performance guarantees under future uncertainty.

In this paper, we propose such a framework for a utility to perform price-based control of flexible building load within the utility's service area, in order to attain competitive performance guarantees in terms of controlling the system peak demand. We note that such

e-Energy '22, June 28-July 1, 2022, Virtual Event, USA

ACM ISBN 978-1-4503-9397-3/22/06…$15.00
https://doi.org/10.1145/3538637.3538836

guarantees would be difficult to attain if buildings are *completely free* to decide on their load. If that is the case, then even when the utility issues very high price incentives, the buildings may refuse to adjust their load. In order to circumvent this difficulty, we introduce the notion of "flexibility contract" between the utility and the buildings. At a high level, the flexibility contract specifies how much flexibility a building has, and a reserve price at which the building promises to invoke its flexibility. In this way, the utility knows that, whenever the price incentives hit the reserve price, it can count on the building's flexibility in a manner almost similar to direct-load control. However, this reserve price is meant to be used only *sparingly*; in most situations, the price incentives will be lower than the reserve price, in which case the buildings still retain their autonomy in deciding how they respond to the price signals. In this sense, our flexibility contract is somewhat analogous to the capacity market at the ISO level [12]: it provides the guarantee for resource adequacy at extreme times, but in most normal operations incentives much lower than the reserve price can be used to solicit the response of the building load. In this way, flexibility contract provides us with a foundation to develop price-based control algorithms that can achieve performance guarantees under uncertainty.

Nonetheless, the design of such a price-based demand response framework is still highly non-trivial. We have to not only carefully specify the form of the flexibility contract, but also carefully compute the price incentives to smoothly transition between non-reserve prices and reserve prices, all in the presence of future load/renewable uncertainty. In the rest of the paper, we present such a complete design. First, we use a Virtual Battery (VB) model [17, 18] to specify the amount of flexibility in our flexibility contract. As we will define clearly in Section 2.1, a VB model has only a few parameters (capacity limit, power limits, and dissipation rate). Therefore, the buildings do not need to disclose their detailed internal models, and can thus retain their privacy. By specifying the VB model, the building promises to take any charging/discharging signals within the limit of the VB model, whenever the price incentives hit the reserve price (which actually corresponds to a pair of prices P_{high} and P_{low}, for discharging and charging, respectively). Second, based on such a flexibility contract, we then design algorithms for computing the price signals. We note that our price-based control algorithms must explicitly consider the future uncertainty. That is, if the price signals and the buildings' response were not controlled carefully, later when the input is bad, even if the utility invokes the reserve price, the buildings may not have any flexibility left! To capture this requirement, we use an uncertainty set to model the uncertainty of future inputs, and we aim to design online price-based control algorithms that can attain a provably-low competitive ratio (CR). As in [24, 34], the CR measures the worst-case ratio between the system peak demand attained by online control and that of an offline algorithm that knows all future inputs in advance. However, [24, 34] considered a direct-load control setting. Thus, one of our main contributions is to develop online price-based control with similar guarantees.

More specifically, our online price-based control algorithm is designed with the following two-step process. In the first step, we assume that the utility can directly control the charging and discharging decisions of each building's VB, and we develop competitive online algorithms for determining these charging/discharging decisions. Towards this end, we aggregate individual buildings' VB into an aggregated VB, which can be viewed as the overall flexibility in the system. We then only need to decide the aggregate charging and discharging decisions to the aggregate VB. Although this aggregation may lose some flexibility, it enables us to design competitive online algorithms with provable CR. Our competitive online algorithms in this setting generalize the idea of [24, 34] to consider both charging/discharging and dissipation.

Then, in the second step, we compute price-signals to achieve the the same aggregate charging/discharging decisions as that of the first step, while allowing the buildings to respond to price-signals based on their own preference. Since the utility does not know the detailed models of the buildings, we model the buildings' preference by their payoff functions (unknown to the utility), formulate an optimization problem to maximize the total system payoff, and then develop distributed solutions for the utility and buildings that converge to the optimal price signals and charging/discharging decisions, respectively. As we discussed earlier, a new difficulty in our setting is that, if the buildings' decisions at an earlier time are not monitored carefully, they may exhaust their flexibility at a future time, which will make our CR guarantee invalid (see detailed example in Section 4). To overcome this difficulty, in Section 4 we introduce a new sufficient condition into our formulation, so that the aggregate flexibility in the system is always maintained. In this way, our distributed price-based control is guaranteed to attain the same CR as that in the first step. Finally, using the idea of robustification from [34], we derive in Section 5 a price-based control algorithm that not only attains a provably-low CR in the worst case, but also attains good average-case performance.

2 SYSTEM MODEL

We assume that time is slotted and indexed by $t = 1, ..., T$ (e.g., T could correspond to 24 hours of a day). We consider a single utility company serving N buildings with demand flexibility. Further, the utility also serves other load and has renewable generation. We further assume that the renewable energy itself cannot fully support all the loads, and thus the utility must always draw energy from the main grid to balance the demand. The goal of the utility is to utilize the flexibility of the buildings to reduce the peak demand drawn from the grid. For simplicity, we subtract the renewable energy from the non-building load at each time t, and denote it by ψ_t. (In this paper, we assume that non-building load is not flexible. This assumption could be relaxed by assuming that they can also be modeled by the VB model to be defined below.)

2.1 Building flexibility and VB model

As we discussed earlier, the HVAC part of a building constitutes a thermal-controllable load (TCL), which can offer significant flexibility. However, we do not want the utility to directly control or observe the buildings' HVAC systems. Instead, we use a flexibility contract to define the amount of flexibility that a building can offer to the utility. A key component of our proposed flexibility contract is the virtual battery (VB) model, which was introduced in [17, 18] and defined below. Let u_t denote the amount of energy charged or discharged to the virtual battery. The specification of VB describes the set of u_t that it can accommodate.

Definition 2.1. [Virtual Battery (VB) Model] A Virtual Battery Model $\mathcal{B}(\Delta, m_-, m_+, a)$ is a set of signals u_t that satisfy:

$$-m_- \le u_t \le m_+, \forall t > 0, \quad (1)$$

$$x_{t+1} - x_t = -ax_t + u_t, x_0 = 0 \Rightarrow -\Delta \le x_t \le \Delta, \forall t > 0. \quad (2)$$

Here, the parameters Δ, m_-, m_+ and a respectively denote the VB's energy capacity, discharging power limit, charging power limit, and its dissipation rate. The variable x_t denotes the State of Charge (SoC) of the VB. Note that even if the (dis)charging decision u_t is zero, the SoC of the VB will drift towards zero. This models the fact that, when only the baseload energy consumption is incurred, the building's internal temperature should gradually approach the nominal temperature set-point (see [17, 18]). Since the SoC maps to the building's internal temperature (see [17, 18]), the SoC will also drift towards zero. The dissipation factor a in (2) captures this effect. Specifically, the update of SoC in formula (2) depends on not only u_t, but also the current SoC and the dissipation factor through the term $(1-a)x_t$. This model however does not account for the charging/discharging efficiency in physical batteries [28], which we leave for future work. According to [19], under certain setting the charging power limit m_+ can be much larger than the discharging power limit m_-. In the rest of the paper, we will assume that m_+ is ∞. We will discuss the impact of this assumption in Section 3.2. Note a small difference from the original definition in [17, 18]: we use $+u_t$ rather than $-u_t$ in (2). In other words, we adopt the more intuitive convention that a fully charged VB will have SoC equal to Δ (instead of $-\Delta$ in [17, 18]).

With such a VB model, we can then separate the energy consumption e_t^i of a building $i (i = 1, ..., N)$ at time t into two parts, its based load b_t^i and the (dis)charging signal u_t^i to its VB, i.e., $e_t^i = b_t^i + u_t^i$. Here, by base-load, we refer to the load of the building without invoking any flexibility (which corresponds to the nominal power P_0^k of TCLs in [17, 18] for maintaining a nominal internal temperature) plus non-HVAC load). Thus, if the building only uses its base-load, the SoC of its VB will always remain at 0. On the other hand, The SoC can increase or decrease when the building invokes its flexibility (i.e., charges or discharges the VB), which usually corresponds to the building's internal temperature deviating from its nominal temperature [17, 18].

Our proposed flexibility contract between the utility and the building includes the specification of the VB model and a pair of reserve prices P_{high} and P_{low}. When a building declares that its VB is $\mathcal{B}^i = \mathcal{B}(\Delta^i, m_-^i, \infty, a^i)$, it promises to take any (dis)charging signals $u_t^i \in \mathcal{B}(\Delta^i, m_-^i, \infty, a^i)$, whenever the price signal given by the utility is P_{high} (for $u_t^i < 0$) or P_{low} (for $u_t^i > 0$).

Note that at each time t, the utility can only observe the total building load e_t^i. Thus, we need a way for the building to declare which part of e_t^i is the base-load. For this purpose, our flexibility contract specifies that, at day-ahead, the building i must declare its predicted range of base-load b_t^i in the form of $[\underline{b_t^i}, \overline{b_t^i}]$. Then, at each time t, the building i must declare its base-load b_t^i within this range. Note that this range should be reasonably small; otherwise the building may be able to disguise its base-load uncertainty as flexibility. The exact limit of this prediction range can be negotiated between the utility and the buildings when the flexibility contact is established.

2.2 Uncontrollable load and uncertainty set

Recall that the uncontrollable load ψ_t includes the non-building load minus the renewable. Since renewable generation has significant uncertainty, we model the uncertainty of ψ_t by an uncertainty set. Specifically, at day-ahead, the utility is given a predicted range $[\underline{\psi_t}, \overline{\psi_t}]$. Then, at time t, the exact value of $\psi_t \in [\underline{\psi_t}, \overline{\psi_t}]$ is revealed to the utility. Further, some of the algorithms that we will discuss later also utilize some predicted value of ψ_t (or b_t^i) at time before t. For that purpose, we simply take the midpoint of $[\underline{\psi_t}, \overline{\psi_t}]$ and $[\underline{b_t^i}, \overline{b_t^i}]$ as the predicted value of ψ_t and b_t^i, respectively.

2.3 Price-based control

Let p denote the nominal price (i.e., with no incentive), and let λ_t^i denote the price incentive to building i at time t. (Thus, the price seen by building i at time t becomes $p + \lambda_t^i$.) Note that when $P_{\text{low}} < p + \lambda_t^i < P_{\text{high}}$, building i is free to choose its response. In this paper, we model such response by a payoff function that is known only to building i, but not to the utility. Specifically, let $U_t^i(e_t^i)$ denote the payoff to building i when its consumption at time t is e_t^i. When the price $p + \lambda_t^i$ at time t has not hit P_{high} or P_{low} yet, building i will choose the decision e_t^i that maximizes its total payoff from current time t to the end of time-horizon T (see line 3 of algorithm in Section 4.2 for details). On the other hand, if the price hits P_{high} or P_{low}, the utility will instruct the building i with the desired value of e_t^i (which must respect building i's VB limits).

2.4 Online algorithms

In practice, both b_t^i and ψ_t are revealed sequentially in time. Therefore, we need an *online* algorithm to determine the price incentives λ_t^i at each time t. We first summarize the information available to our online algorithm.

At day-ahead (or equivalently time 0), the utility is given $Y = \{\underline{b_t^i}, \overline{b_t^i}, \underline{\psi_t}, \overline{\psi_t}, t = 1..T\}$ and each building's own VB: $\mathcal{B}^i = \mathcal{B}(\Delta^i, m_-^i, \infty, a^i)$, $i = 1..N$. Also, the utility will announce the nominal price p. At any time $t = 1, ..., T$, building i declares its real-time baseload b_t^i. Further, the utility is given the uncontrollable load ψ_t. Then, after receiving the price incentive λ_t^i from the utility, the building controls its total consumption e_t^i, which can be measured by the utility. Each building's current SoC(i.e., x_t^i) can then be updated by the values of b_t^i and e_t^i at time.

With this set-up, the price incentive computed by the utility at time t can only depend on information that has been revealed before time t. Specifically, let $Z_t = [b_s^i, \psi_s, s = 1, 2, ..., t]$. Then, λ_t^i must be a function of Y and Z_t. At the end of the time horizon T, the utility knows all revealed demand $Z = [b_s^i, \psi_s, s = 1, 2, ..., T]$. We refer to Z as a realization, which is only revealed at time T.

In this paper, we assume that Y is given, because it is known day-ahead. The uncertainty comes from the realization Z. Even though we do not know the exact realization in advance, the knowledge of Y helps restrict the search space into a smaller set, i.e.,

$$Z_Y = \{Z | Z = [b_s^i, , x_s^i, s = 1, ..., T] \text{ such that it is consistent with Y}\}$$

At each time t, we can write any possible future realization $Z \in Z_Y$ as $Z = [Z_t, Z_{>t}]$, where $Z_{>t}$ denotes the elements of Z that will be

revealed after time t. In summary, at each time our online algorithm π must map from Y and Z_t to λ_t^i, even though it does not know $Z_{>t}$ yet.

2.5 Objective

Under an online algorithm π, for each realization $Z \in Z_Y$, it will lead to a sequence of building load $e_t^i(Z_t, \pi)$. (Note that here we have added Z_t in the notation to emphasize that both the decision of π and the resulting e_t^i only depends on information revealed before time t.) Our goal is to minimize the system peak demand drawn from the grid, which is given by $E_\pi^{\mathrm{p}}(Z) = \max_{t=1,\ldots,T} \left(\sum_i e_t^i(Z_t, \pi) + \psi_t\right)$.

Let $E_{\mathrm{off}}^*(Z)$ be the system peak demand under a suitably-chosen optimal offline solution. Obviously, for any online algorithm, we must have $E_{\mathrm{off}}^*(Z) \le E_\pi^p(Z)$. The competitive ratio [34] of an online algorithm π is the maximum ratio between $E_\pi^p(Z)$ and $E_{\mathrm{off}}^*(Z)$ under all possible realizations, i.e., $\eta_Y(\pi) = \max_{Z \in Z_Y} \frac{E_\pi^p(Z)}{E_{\mathrm{off}}^*(Z)}$. Our goal is to achieve a provably low competitive ratio. In the next two sections, we will develop such a solution.

3 ONLINE ALGORITHM UNDER DIRECT-VB CONTROL

Recall that our proposed solution will be developed in two steps. In this section, we tackle the first step, i.e., to develop competitive online algorithms assuming that the utility can directly charge/discharge the VBs. Then, in the next section, we will convert the algorithm from direct-VB control to price-based control. Below, we first present the offline solution that we use as a reference to compute the competitive ratio, and then provide an online algorithm that can attain the best possible competitive ratio under direct-VB control setting.

3.1 Aggregate VB and offline optimal solution

We borrow the ideas from the EPS algorithm in [34] to develop our competitive online algorithms under this direct-VB control setting. Unfortunately, the methods in [34] cannot directly work with multiple VBs. Thus, to make progress, we use the concept of an aggregate VB introduced in [17, 18]. Specifically, given a set of $\beta_i^0 > 0$ such that $\sum_i \beta_i^0 = 1$, the aggregate VB $\mathcal{B}(C, m_-, \infty, a)$ is given by the following relationship:

$$C = \min_{i=1,\ldots,N} \frac{f^i}{\beta_i^0},\ m_- = \min_{i=1,\ldots,N} \frac{m_-^i}{\beta_i^0}, \qquad (3)$$
$$f^i := \Delta^i/(1 + |1 - a/a^i|).$$

Note that the parameter β_i^0 can be viewed as the fraction of u_t that is sent to VB i at time t, i.e., $u_t^i = \beta_i^0 u_t$. The constraints in (3) ensure that the limits of the individual VBs are always respected. Note that according to the derivation in [17, 18], when $a = a^i = 0$, the last expression is simply $f^i = \Delta^i$. The value of β_i^0's may be chosen according to certain optimization objectives (see [17, 18]).

Since we have already aggregated all VBs into one, we also define $B_t = \sum_i b_t^i$ and $E_t = \sum_i e_t^i + \psi_t$ as the aggregate baseload and aggregate consumption, respectively, of all buildings. (According to the meaning of β_i^0, it is implied that the building i's actual consumption will be $\beta_i^0(E_t - B_t - \psi_t) + b_t^i$.)

Based on this aggregate VB, we can then define the offline optimal solution to minimize the system peak demand:

$$E_{\mathrm{off}}^*(Z) = \min \max_{t=1,\ldots,T} \{E_t\},$$
$$\text{sub to } -m \le E_t - B_t - \psi_t,\ t = 1, \ldots T,$$
$$-C \le \sum_{s=1}^{t} (1-a)^{t-s}(E_s - B_s - \psi_s) \le C,\ t = 1, \ldots, T.$$

In the rest of the paper, our competitive ratio will be defined with respect to this offline optimal solution.

The following lemma, which is essential for deriving the optimal competitive online algorithm, provides a sufficient and necessary condition for any sequence of $[E_1, \ldots, E_t]$ (which we refer to as a profile) to be feasible. See Appendix B for the proof.

Lemma 3.1. *Given a demand realization Z, a sufficient and necessary condition for a profile $[E_1, \ldots, E_T]$ to be feasible, i.e., all charging and discharging signals respect the aggregate VB limits, is that all of the following inequalities hold for any $t_2 \ge 1$:*

$$\sum_{t=1}^{t_2} (1-a)^{t_2-t}(B_t + \psi_t) - C \le \sum_{t=1}^{t_2} (1-a)^{t_2-t} E_t$$
$$\le \sum_{t=1}^{t_2} (1-a)^{t_2-t}(B_t + \psi_t) + C, \qquad (4)$$
$$b_{t_2} + \psi_{t_2} - m_- \le E_{t_2}, \forall t_2. \qquad (5)$$

Equation (4) essentially ensures that, starting with SoC = 0 at time 0, after serving all baseloads and uncontrollable load, the power signal applied to the aggregated battery must respect the capacity constraint at any time $t_2 > 0$. Similarly, Equation (5) ensures that the discharging limit is met at all times.

Remark: Creating a new version of (4) by replacing t_2 with $t_1 - 1$, multiplying by $(1-a)^{t_2-t_1+1}$ and then subtracting the original version of (4), we obtain the following necessary condition for any $1 < t_1 \le t_2 \le T$ (Please see Appendix E for the detailed derivation):

$$\sum_{t=t_1}^{t_2} (1-a)^{t_2-t}(B_t + \psi_t) - C - C(1-a)^{t_2-t_1+1} \le \sum_{t=t_1}^{t_2} (1-a)^{t_2-t} E_t$$
$$\le \sum_{t=t_1}^{t_2} (1-a)^{t_2-t}(B_t + \psi_t) + C + C(1-a)^{t_2-t_1+1}. \qquad (6)$$

They are also intuitive to interpret. The first (resp. second) inequality states that, starting from SoC = C (resp. SoC = $-C$) at time t_1, the SoC at time t_2 should not be lower than $-C$, i.e., no over-discharge (resp. should not be higher than $+C$, i.e., no overcharge).

3.2 Lower bound on the optimal CR

Consider an online algorithm π with competitive ratio (CR) $\eta_Y(\pi)$, and let $E_t(Z_t, \pi)$ be its decision for the aggregate building consumption E_t at time t. Recall that the decision $E_t(Z_t, \pi)$ should only depend on Z_t. Given Z_t, there may be multiple realizations Z' with the same prefix up to time t. Define the *peak estimate* as the *lowest* offline optimal system peak among all such realizations Z' with the prefix Z_t, i.e.,

$$E_t^{\mathrm{pe}}(Z_t) = \inf_{Z' \in Z_Y : Z'_t = Z_t} E_{\mathrm{off}}^*(Z'). \qquad (7)$$

Clearly, we must have $E_t(Z_t, \pi) \le \eta_Y(\pi) E_t^{\text{pe}}(Z_t)$. Otherwise, if the realization Z' that minimizes (7) occurs, the system peak under algorithm π will violate the CR $\eta_Y(\pi)$.

We can now apply Lemma 3.1. If π is feasible, then for all $Z \in Z_Y$ and $1 < t_1 \le t_2 \le T$, we must have, from (6):

$$\sum_{t=t_1}^{t_2}(1-a)^{t_2-t}(B_t+\psi_t) - C - C(1-a)^{t_2-t_1+1} \le \sum_{t=t_1}^{t_2}(1-a)^{t_2-t}E_t \le \eta_Y(\pi)\sum_{t=t_1}^{t_2}(1-a)^{t_2-t}E_t^{\text{pe}}(Z_t). \quad (8)$$

We thus have $\eta_Y(\pi) \ge \frac{\sum_{t=t_1}^{t_2}(1-a)^{t_2-t}(B_t+\psi_t)-C-C(1-a)^{t_2-t_1+1}}{\sum_{t=t_1}^{t_2}(1-a)^{t_2-t}E_t^{\text{pe}}(Z_t)}$. Since this inequality must hold for all Z, we can define the following optimization problem: $\forall 1 < t_1 \le t_2 \le T$,

$$\eta^*_{t_1,t_2,C}(Y) = \sup_{Z\in Z_Y} \frac{\sum_{t=t_1}^{t_2}(1-a)^{t_2-t}(B_t+\psi_t) - C - C(1-a)^{t_2-t_1+1}}{\sum_{t=t_1}^{t_2}(1-a)^{t_2-t}E_t^{\text{pe}}(Z_t)}. \quad (9)$$

We must then have $\eta_Y^* \ge \max_{\forall 1<t_1\le t_2\le T} \eta^*_{t_1,t_2,C}(Y)$.

Similarly, using (4) and (5), we can define additional lower bounds as the solutions of the following optimization problems.

$$\eta^*_{1,t_2,C}(Y) = \sup_{Z\in Z_Y} \frac{\sum_{t=1}^{t_2}(1-a)^{t_2-t}(B_t+\psi_t) - C}{\sum_{t=1}^{t_2}(1-a)^{t_2-t}E_t^{\text{pe}}(Z_t)}, \forall t_2 \le T$$

$$\eta^*_{t_2,m_-} = \sup_{Z\in Z_Y} \frac{(b_{t_2}+\psi_{t_2}) - m_-}{E_{t_2}^{\text{pe}}(Z_{t_2})}, \forall 1 \le t_1 \le t_2 \le T. \quad (10)$$

We then have the following theorem, which provides the tightest lower bound on the optimal competitive ratio (CR).

Theorem 3.2. *For any feasible online algorithm, its competitive ratio must be no smaller than* $\eta_Y^* = \max\Big\{\max_{1<t_1\le t_2\le T}\eta^*_{t_1,t_2,C}(Y), \max_{1<t_1\le t_2\le T}\eta^*_{1,t_2,C}(Y), \max_{1\le t_1\le t_2\le T}\eta^*_{t_1,t_2,m_-}(Y)\Big\}$.

Note that the optimization problem (9) itself is not convex. Nonetheless, we can convexify the optimization problem (9) using the convexification method in [34]. Therefore, it can be solved with any convex optimization solver.

Remark: Note that in deriving (8), we only used the first part of the inequality (6) (i.e., no over-discharge). It turns out that, when $m_+ = \infty$, this is sufficient for the purpose of deriving the optimal online algorithm in the next subsection. For future work, it would be of interest to study the case $m_+ < \infty$.

3.3 EPS algorithm with the optimal CR

We next present an algorithm that achieves the CR lower bound η_Y^*. Specifically, we use the idea of EPS (Estimated Peak Scaling) algorithm in [34], which sets the value of E_t to be $\eta_Y^* E_t^{\text{pe}}(Z_t)$ (i.e., it multiplies the current peak estimate by η_Y^*). However, the caveat is that the utility also needs to check whether the aggregate VB is overcharged, which is important because our derivation of (9) has not considered the no-overcharge part of (6). If overcharging indeed happens (after serving baseload and uncontrollable load), the EPS algorithm should reduce E_t to be the amount that only charges the VB to full (i.e., E_t is reduced to $C - (1-a)x_t + B_t + \psi_t$).

The following theorem then states that the EPS algorithm attains the optimal competitive ratio η_Y^*. Note that the second part of Theorem 3.3 is crucial because, when $E_t < \eta_Y^* E_t^{\text{pe}}(Z_t)$, it is no long clear why (8) can still hold, i.e., no over-discharging occurs. The proof below eliminates this doubt. See Appendix C for the proof.

Theorem 3.3. *The EPS algorithm satisfies the following two requirements, for any realization* $Z \in Z_Y$*:*

1) At each time slot t*, the aggregate energy consumption* E_t *satisfies* $E_t \le \eta_Y^* E_{\text{off}}^*(Z)$.

2) The constraints of the aggregate VB are obeyed at all times.

Remark: Our methodology in this section is similar to [24, 34]. However, [24, 34] considers either charging or discharging, but not both, and neither of them study dissipation. Thus, our main contribution here is in extending the methodology to account for all three factors.

4 PRICE-BASED CONTROL

In this section, we proceed to the second step of our solution, i.e., we will develop a new price-based control algorithm where the utility only sends out price signals. Thus, buildings make their own charging/discharging decisions as a response to the price signals. As we discussed in Section 2.3, we model the building's response as the solution to a payoff maximization problem, which will be made precise in (11).

Here, we assume that, at time t, the utility has computed the aggregated consumption decision E_t. We refer to the sequence $[E_1, ..., E_T]$ as the aggregate profile. E_t could be computed by the method of Section 3 assuming direct-VB control[1]. Our goal in this section is to ensure that, whatever aggregate profile that the utility wishes to attain assuming direct-VB control, the price-based control will produce the same aggregate profile, even when buildings make decisions distributively. Recall that direct-VB control in Section 3 essentially assumes that each VB will be charged/discharged according to β_i^0 in (3). Thus, one new challenge is that, since the buildings' distributed decisions may deviate from that of direct-VB control, demand flexibility may be depleted in such a way that, at a future time, the above guarantee (i.e., price-based control attains the same aggregate profile as direct-VB control) would no longer be feasible. The key contribution of this section is therefore to provide a new sufficient condition that prevents such an adverse scenario from ever occurring, so that the above guarantee will hold even under future load uncertainty and when the utility has no knowledge of the internal payoff functions of the buildings.

Below, we will first introduce a centralized formulation to model the objective and constraints of this price-based control framework. Then, we will specify an iterative algorithm so that the price signals and buildings' response can be computed distributively by the utility and buildings, where each party has only limited knowledge of the internal operations of other parties.

4.1 A centralized formulation

Recall we assume that at each time t the utility already computes the aggregate decision E_t. Under direct-VB control, the utility can

[1] In Section 5, we show that the decisions of Section 3 can be further improved, in which case the method of this section can still be applied.

Table 1: An example of infeasibility when buildings choose their own charging/discharging decisions.

Time Slot	$t=0$	$t=1$	$t=2$	$t=3$
Direct-VB control Decision (u_t^1/u_t^2)		-1.5/-1.5	-1/-1	-2/-2
Accumulated Charge under Direct-VB control (x_t^1/x_t^2)	0/0	-1.5/-1.5	-2.5/-2.5	-4.5/-4.5
Individual Decision (u_t^1/u_t^2)		-3/0	-2/0	Infeasible
Accumulated Charge under Individual Decision (x_t^1/x_t^2)	0/0	-3/0	-5/0	Infeasible

simply split E_t to each building by $e_t^i = \beta_i^0(E_t - B_t - \psi_t) + b_t^i$. In contrast, for price-based control, the buildings' charging/discharging decision may deviate from the above direct-VB control decision. Still, we want to guarantee that the buildings' decision will also satisfy $\sum_i e_t^i + \psi_t = E_t$ at all time. However, this is challenging because, if at an earlier time the buildings' decisions deviate arbitrarily, they may deplete the flexibility of the VBs in such a way that the overall system state is driven to an extreme point. Then, at a later time, there may not exist feasible decisions that can both satisfy $\sum_i e_t^i + \psi_t = E_t$ and respect each VB's individual limits. Next, we provide a counter example to illustrate this difficulty.

A Counter Example: Suppose that we have two buildings that are modelled as VBs. The maximum accumulated charge that each VB can hold is 5, and the discharging power limit of each VB is 3. There is no dissipation (i.e., $a = 0$). Using the method of [17, 18], the utility can aggregate these two VBs into a single VB, e.g., one that can hold a maximum charge of 9, and whose discharging power limit is 4. Suppose that, at time slots 1, 2 and 3, the utility needs the aggregate VB to discharge 3, 2 and 4, respectively. It is easy to verify that this sequence of decisions can be achieved by direct-VB control, while respecting individual VB's limits. Indeed, as the second row of Table 1 shows, the utility can simply split the discharging decision evenly between the two VBs (e.g., "-1.5/-1.5" in time slot 1 means that the first VB is discharged 1.5 and the second VB is also discharged 1.5). The third row shows that both VBs' total accumulated charges are with their capacity limits. However, if buildings are allowed to choose their own discharging decisions, they may choose the decisions in the fourth row. Specifically, in time-slots 1 and 2, even though the total discharge decision is still the the same as that of the first row, only building 1 discharges its VB. The corresponding total accumulated charges are shown in the fifth row. Now, at time-slot 3, when the utility wants to discharge another 4, there is no longer a feasible solution for charging the VBs: building 1 is already empty and cannot take any more discharge, while building 2 can at most discharge 3 because of its discharging power limit. As we have seen, a sequence of aggregate discharging decisions that was feasible under direct-VB control is no longer feasible when buildings choose their own decisions.

New Sufficient Condition: Clearly, in order to ensure that price-based control can attain the same sequence of aggregate decisions as direct-VB control, we need some additional restrictions on how buildings charge/discharge their individual VBs at each time. Below, we introduce a new sufficient condition that eliminates the above infeasibility problem for the future. Recall that the VB model of building i is $\mathcal{B}^i = \mathcal{B}(\Delta^i, m_-^i, \infty, a^i)$. In (3), the utility has computed an aggregate VB of parameter $\mathcal{B}(C, m_-, \infty, a)$. Suppose that the current time is t_c. Our new condition will ensure that, if the buildings' decisions $e_{t_c}^i$ at time t_c satisfy this condition, then for any sequence of future aggregate decisions $E_t, t > t_c$ that can be supported by the aggregate VB $\mathcal{B}$, there always exist buildings' individual decisions e_t^i that respect the individual VBs' limits and that add up to $E_t - \psi_t$.

Specifically, let $x_{t_c-1}^i$ denote the SoC for individual VB $\mathcal{B}^i$ at time slot $t_c - 1$. Let x_{t_c-1} denote the SoC for the aggregate VB at time slot $t_c - 1$. Recall that $e_{t_c}^i$ is the energy consumption of building i, which should add up to $E_{t_c} - \psi_{t_c}$. We have the following theorem.

Theorem 4.1. *Suppose that the following conditions are satisfied for some $\beta_i \geq 0$, $i = 1, ..., N$:*

$$\Big|[(1-a^i)x_{t_c-1}^i + (e_{t_c}^i - b_{t_c}^i)] - \beta_i[(1-a)x_{t_c-1} + (E_{t_c} - \psi_{t_c} - B_{t_c})]\Big| + \beta_i\Big(1 + \left|\frac{a-a^i}{a}\right|\Big)C \leq \Delta^i,\ i = 1...N,$$

$$\beta_i \cdot m_- \leq m_-^i,\ i = 1...N,\ \text{and}\ \sum_{i=1}^N \beta_i = 1.$$

Then, for any future aggregate profile $[E_t, t > t_c]$ that the utility decides to use and that satisfies the aggregate VB constraints $\mathcal{B}$, there always exists individual buildings' decisions e_t^i for future t such that $E_t = \sum_i e_t^i + \psi_t$ and their individual VBs' limits are respected.

See Appendix D for the detailed proof. In Theorem 4.1, β_i can be thought of as the fraction of future aggregate charge/discharge decision (i.e., $E_t - B_t - \psi_t$) that will be sent to building i, i.e., $e_t^i = \beta_i(E_t - B_t - \psi_t) + b_t^i$ for $t > t_c$. Assuming such a constant splitting, the first constraint ensures that the individual VB's capacity limit Δ^i is respected. The second constraint ensures that the individual VB's discharging power limit is respected. The final constraint ensures that the decisions e_t^i of the buildings always add up to $E_t - \psi_t$.

We note that β_i is similar to, but different from, β_i^0 that was used to compute the aggregate VB in (3). Specifically, according to [17, 18], if $e_t^i = \beta_i^0(E_t - B_t - \psi_t) + b_t^i$ for all t, then the individual decisions e_t^i always respect VB limits. However, under distributed control, at time t_c building i's decision $e_{t_c}^i$ may deviate from the above value. As a result, using the same β_i^0 may not work for the future. That is why the value of β_i in Theorem 4.1 will usually differ from β_i^0 (and they also change with t_c).

Centralized Formulation: Based on the above sufficient condition, we can then formulate the following centralized optimization problem **PC** at time t_c, based on which we will develop the distributed price-based control algorithm.

$$\textbf{PC}: \max_{[e_t^i],[\beta_i]} \sum_{t=t_c}^{T}\sum_{i=1}^{N} U_t^i(e_t^i) - p\sum_{t=t_c}^{T}\sum_{i=1}^{N} e_t^i - \sum_{i=1}^{N}(\beta_i - \beta_i^0)^2 \tag{11}$$

$$\text{sub to}\ \sum_{i=1}^{N} e_{t_c}^i = E_{t_c} - \psi_t, \tag{12}$$

$$-m_-^i \leq e_t^i - b_t^i, t = t_c, ...T, i = 1, ..., N,$$

Algorithm 1: Price-based Distributed Algorithm

1: **repeat**

2: Each building i receives the current iteration price of $p^i_{t_c}(k) = p + \lambda_{t_c}(k) + \mu^i_{t_c,1}(k) - \mu^i_{t_c,2}(k)$ from utility;

3: Based on the current values of the dual variables, each building i chooses a new energy consumption decision $e^i_t(k), t \geq t_c$, which is the solution of the following optimization problem:

$$\textbf{PB}: \max_{[e^i_t]} \sum_{t=t_c}^{T} U^i_t(e^i_t) - p^i_{t_c}(k) e^i_{t_c} - p \sum_{t=t_c}^{T} e^i_t$$

$$\text{sub to} \quad -\Delta^i \leq \sum_{j=1}^{t} (1-a^i)^{t-j}(e^i_j - b^i_j) \leq \Delta^i, \forall t \geq t_c$$

$$-m^i_- \leq e^i_t - b^i_t, \; t = t_c, \ldots T.$$

4: Based on the current values of the dual variables, the utility determines β_i by solving the following optimization problem:

$$\textbf{PU}: \max_{[\beta_i]} \sum_{i=1}^{N} \beta_i \mu^i_{t_c,1}(k) \left[|1 + \frac{a-a^k}{a}| C - (1-a) x^i_{t_c-1} - E_{t_c} \right] + \sum_{i=1}^{N} \beta_i \mu^i_{t_c,2}(k) \left[(1-a) x^i_{t_c-1} + |1 + \frac{a-a^k}{a}| C + E_{t_c} \right]$$

$$- \sum_{i=1}^{N} (\beta_i - \beta^0_i)^2$$

$$\text{sub to} \quad \beta_i \cdot m_- \leq m^i_-, \; i = 1 \ldots N \text{ and } \sum_{i=1}^{N} \beta_i = 1$$

5: Building i communicates $e^i_{t_c}(k)$ to the utility;

6: Based on $e^i_{t_c}(k)$, the utility updates the new dual variables by:

$$\lambda_{t_c}(k+1) = \left[\lambda_{t_c}(k) + \gamma \big(\sum_i e^i_{t_c}(k) + \psi_{t_c} - E_{t_c} \big) \right]^+$$

$$\mu^i_{t_c,1}(k+1) = \left[\mu^i_{t_c,1}(k) + \gamma_1 \Big[e^i_{t_c}(k) - b^i_{t_c} + \beta_i \big[|1 + \frac{a-a^k}{a}| C - (1-a) x_{t_c-1} - (E_{t_c} - B_{t_c} - \psi_{t_c}) \big] - \Delta^i + (1-a) x^i_{t_c-1} \Big] \right]^+$$

$$\mu^i_{t_c,2}(k+1) = \left[\mu^i_{t_c,2}(k) + \gamma_2 \Big[\beta_i \big[|1 + \frac{a-a^k}{a}| C + (1-a) x_{t_c-1} + (E_{t_c} - B_{t_c} - \psi_{t_c}) \big] - \Delta^i - (1-a) x^i_{t_c-1} - (e^i_{t_c}(k) - b^i_{t_c}) \Big] \right]^+$$

where $[x]^+ = \max\{x, 0\}$, and $\gamma, \gamma_1, \gamma_2 > 0$ are the step sizes;

7: **until** The above iteration converges, i.e., when $\sum_i e^i_{t_c}(k) + \psi_{t_c}$ is sufficiently close to E_{t_c}

$$-\Delta^i \leq \sum_{j=1}^{t} (1-a^i)^{t-j}(e^i_j - b^i_j) \leq \Delta^i, \forall t \geq t_c, \forall i,$$

$$\beta_i \cdot m_- \leq m^i_-, i = 1 \ldots N, \text{ and } \sum_{i=1}^{N} \beta_i = 1,$$

$$\Big| [(1-a^i) x^i_{t_c-1} + (e^i_{t_c} - b^i_{t_c})] - \beta_i [(1-a) x_{t_c-1} + (E_{t_c} - \psi_{t_c} - B_{t_c})] \Big| + \beta_i \left(1 + \left| \frac{a-a^i}{a} \right| \right) C \leq \Delta^i, \forall i. \tag{13}$$

Here, the objective represents the total payoff of all buildings (where $U^i_t(\cdot)$ is the payoff function of building i for time t), minus the cost of energy (at the nominal price of p), minus a special term $\sum_{i=1}^{N} (\beta_i - \beta^0_i)^2$ that captures the deviation of β_i from β^0_i. In the constraints, the first constraint ensures that the buildings' decision $e^i_{t_c}$ at time t_c add up to E_{t_c}. The second and third constraints allow each building to ensure that its VB's capacity and power limits are met, based on its "expected" future sequence of decisions $e^i_t, \; t > t_c$. Note that here we do not impose the constraint $\sum_i e^i_t = E_t - \psi_t$ for $t > t_c$, because the utility's decisions E_t for future time-slots have not been revealed yet. In the future when the utility's decision E_t is revealed at time t, obviously e^i_t will have to be changed to another value. The last four constraints (from Theorem 4.1) ensure that there always exist such feasible e^i_t at future time t.

4.2 Price-based distributed control algorithm

From Problem **PC**, we can then derive a distributed solution. The highly-desirable feature of this distributed solution is that utility does not even need to know the buildings' internal payoff functions.

In each iteration, utility sends a tentative price/incentive signal to the buildings. After feedback from buildings (i.e., their load adjustment) is received (either via explicit communication messages or via load measurement), utility updates the price signals and sends them again to the building. The process repeats until either convergence or a maximum number of iterations within the time-slot has been reached.

Specifically, suppose that the current time is t_c. Let E_{t_c} be the aggregate energy consumption that the utility wishes to attain at time t_c. Let $\lambda_{t_c}, \mu^i_{t_c,1}$ and $\mu^i_{t_c,2}$ denote the dual variables associated with the constraints (11) and (13) of the centralized optimization problem **PC**. (The constraint (13) can be rewritten as two linear constraints using $x \leq |x|$ and $-x \leq |x|$, and hence there are two dual variables $\mu^i_{t_c,1}$ and $\mu^i_{t_c,2}$.) Using standard duality theory [8], we can then obtain Algorithm 1, which describes its k-th iteration.

Further, using standard duality theory, we can show that the above iterative algorithm will converge to the solution to (11), provided that the stepsizes are sufficiently small. Note that in problem **PB** for each building, $p + \lambda_{t_c}(k) + \mu^i_{t_c,1}(k) - \mu^i_{t_c,2}(k)$ can be viewed as the new price for building i and time-slot t_c at iteration k. This price signal is the only information that building i needs to receive from the utility in order to compute its consumption $e^i_{t_c}$. Similarly,

in problem **PU**, the utility only needs to receive the consumption $e^i_{t_c}(k)$ from building i, and does not need to know the internal parameters of the buildings. Hence, this distributed algorithm is easy to implement and incurs low communication overhead.

4.3 Using the reserve price

The above algorithm will work if all buildings respond adequately to the price signals. However, since we allow the buildings to make their own decisions, it may also occur that some buildings may not respond adequately. Recall that we have the reserve prices P_{high} and P_{low}, at which point the building must discharge or charge according to the amount specified by the utility, as long as the SoC is still within the VB limits. Still, we need a way to detect these buildings and compute the decision that the utility should send them along with the reserve prices.

Specifically, when utility updates the price of each building in Line 6, the prices of those buildings who do not respond adequately will be higher or lower than others. Thus, those buildings will typically hit the reserve price earlier than others. Once the prices $p + \lambda_{t_c}(k) + \mu^i_{t_c,1}(k) - \mu^i_{t_c,2}(k)$ of some buildings reach the reserve prices, the utility can now directly calculate its energy consumption $e^i_{t_c}$ using the value of β_i calculated at the previous time slot, and send this consumption decision along with the reserve price to this subset of buildings. For the rest of buildings, they can still run the above distributed algorithm until convergence, or when their prices also hit the reserve prices, in which the above procedure is followed again. (In case such buildings still do not follow the decision from the utility, they are considered in violation of the flexibility contracts. If that happens, additional penalty may be imposed as negotiated for the flexibility contract.)

5 ALGORITHM ROBUSTIFICATION

The solution framework in Section 4 can convert the decisions E_t by any online algorithm under the direct-VB control setting to distributed price-based control. As a result, it will attain the same aggregate energy consumption E_t and thus the same competitive guarantee. For instance, we could directly use the decisions by the EPS algorithm in Section 3. However, one issue with EPS is that, although it achieves the optimal CR for the worst-case input, its average-case performance can be poor. This is due to the fact that EPS always takes E_t to be the highest possible value (i.e., $\eta^*_Y E^{\text{pe}}_t$). There may exist other online algorithms that have better average-case performance (e.g. MPC which we will discuss in Section 6). However, they may not have the best competitive guarantees for the worst-case inputs. This dilemma between worst-case performance and average-case performance is common in the context of competitive online algorithms [34]. In the rest of this section, we will use the "robustification" procedure introduced in [34], which takes any online algorithms with good average-case performance into one that achieves both the optimal CR and good average-case performance.

Towards this end, we will first expand EPS into a much larger class of online algorithms, called ABS (Adaptive Bound-based Scheduling), so that any algorithm in ABS will attain the optimal CR η^*. We first derive a necessary condition for any ABS algorithm π. Consider any realization $Z \in Z_Y$. At each time slot t, the upper bound on $E_t(Z_t, \pi)$ is already given by $E_t(Z_t, \pi) \le \eta^*_Y E^{\text{pe}}_t(Z_t)$ (so that if the offline peak is indeed E^{pe}_t, the CR of π will be no greater than η_Y*). We next derive a lower bound on $E_t(Z_t, \pi)$. Suppose that the current SoC of the aggregate VB is x_t. A necessary condition for CR to be η^* can be stated as follows: if the current consumption is E_t, and the future consumption is $\eta^*_Y E^{\text{pe}}_s$ for $s > t$ (i.e., the highest possible consumption is used for all future time), the aggregate VB will never be over-discharged. Specifically, defining $O_t = B_t + \psi_t$ for ease of presentation, we need $(1-a)^{t_1+1-t}x_t + (1-a)^{t_1-t}(E_t - O_t) + \sum_{s=t+1}^{t_1}(1-a)^{t_1-s}(\eta^*_Y E^{\text{pe}}_s(Z_s) - O_s) \ge -C$ for all $t_1 > t$. Note that if we take the convention that $\sum_{s=t+1}^{t} = 0$, this inequality must also hold for $t_1 = t$, i.e., $E_t(Z_t, \pi) - O_t \ge -C - (1-a)x_t$, so that the aggregate VB is not over-discharged at time t. Reorganizing the terms, we must then have, for all $t_1 \ge t$

$$E_t(Z_t, \pi) - O_t \ge \frac{\sum_{s=t+1}^{t_1}(1-a)^{t_1-s}O_t - C}{(1-a)^{t_1-t}} + \frac{-(1-a)^{t_1+1-t}x_t - \eta^*_Y \sum_{s=t+1}^{t_1}(1-a)^{t_1-s}E^{\text{pe}}_s(Z_s)}{(1-a)^{t_1-t}}. \quad (14)$$

Since this inequality must be true for all future realizations, we can maximize the right-hand-side to obtain the best lower bound. Specifically, define the following optimization problem that maximizes the RHS of (14) over all possible future inputs:

$$R^*_{\eta^*_Y}(Z_t, t_1) = \max_{Z' \in Z_Y : Z'_t = Z_t} \text{RHS of (14)}. \quad (15)$$

Therefore, we can obtain the following lower bound for $E_t(Z_t, \pi)$:

$$E_t(Z_t, \pi) \ge \max_{t_1 \ge t}(R^*_{\eta^*_Y}(Z_t, t_1)) + O_t. \quad (16)$$

Further, we should have $E_t(Z_t, \pi) \ge O_t - m_-$ to respect the discharging power limit.

Based on the above lower and upper bounds, we can then define a class of online algorithm, called ABS (Adaptive Bound-Based Scheduling), which at each time t essentially uses any value of E_t between $\eta^* E^{\text{pe}}_t$ and $\max\{\max_{t_1 \ge t}(R^*_{\eta^*_Y}(Z_t, t_1)) + O_t\}, O_t - m_-\}$. We refer the readers to Appendix A for the details of the ABS algorithm.

Finally, using the idea of ABS algorithms, we can then employ the following "robustification" procedure, which converts any online algorithm π_0 with reasonable average-case performance into one in the class ABS (and thus with the optimal CR). That is, if the decision $E_t(Z_t, \pi_0)$ of algorithm π_0 at time t is between the upper and lower bounds, we simply use the same decision as π_0. Otherwise, we "robustify" the decision by setting it to one of the bounds, such that the resulting robustified algorithm belongs to ABS. Finally, note that such a robustified decision can again be used in Section 4 to perform price-based control. In this way, our price-based control will attain both the optimal CR and reasonable average-case performance. See Appendix A for further details of this robustification procedure.

6 SIMULATION RESULTS

In this section, we simulate our proposed solution using both synthetic traces and realistic traces from data sets of Elia [1], Belgium's electricity transmission system operator. In the following, the units for load, consumption E_t and discharging limit is KW, and the unit for capacity is KWh. We will mainly use MPC (Model Predictive Control) [2, 23] as the state-of-art algorithm for comparison. Note

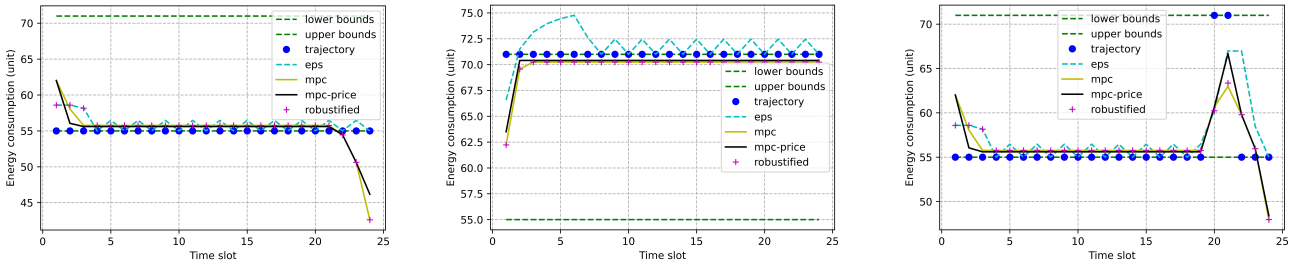

(a) lower bound trajectory (b) upper bound trajectory (c) trajectory with a later peak

Figure 1: Comparison among three scenarios under smaller dissipation (i.e., $a = 0.08$)

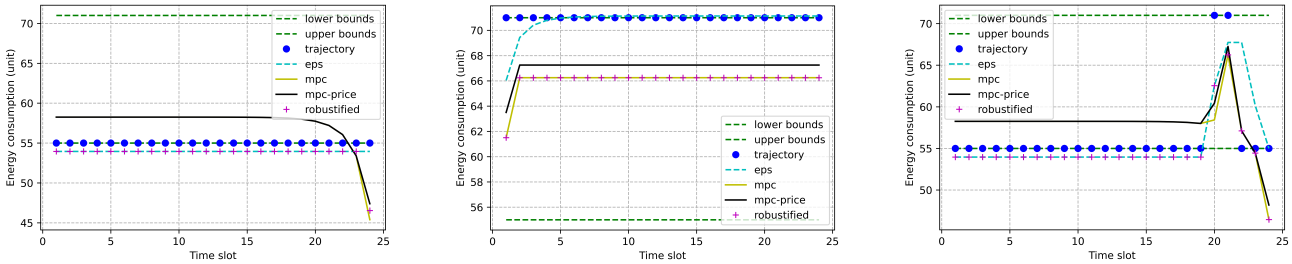

(a) lower bound trajectory (b) upper bound trajectory (c) trajectory with a later peak

Figure 2: Comparison among three scenarios under larger dissipation (i.e., $a = 0.5$)

that while there is a large body of work on price-based demand response, many of them do not deal with future uncertainty in inputs, i.e., they assume that the future inputs (including both load and renewable generation) are known [21, 31]. When key inputs, e.g., future renewable generation, have significant uncertainty, a common way to interpret the above class of algorithms is to use MPC or RHC [2, 23]. Specifically, at each time, assuming that the future inputs are at some predicted values, a decision for the entire time-horizon is computed based on the above-mentioned class of algorithms. Then, only the decision for the current time-slot is executed. In the next time-slot, new input is revealed, and then the above procedure is repeated. As we will explain below, we will compare the performance of our algorithm with two variants of the MPC algorithms.

6.1 Synthetic trace

We first use synthetic traces to study the performance of our proposed solution. While the synthetic traces may be unrealistic, they help us identify patterns in the input that may lead to poor performance under future uncertainty. Since our goal is to provide provable performance guarantee for all inputs (including the worst-case inputs), it is useful to understand what correspond to these worst-case inputs. Even though the exact synthetic traces are unlikely to occur in reality, their patterns do show up in realistic traces, as we will explain later in the next subsection.

We first use the following synthetic trace. There are 4 buildings. The uncertainty set of each building's baseload b_i^t is $[8, 10]$, $[7, 9]$,$[5, 6]$, and $[8, 10]$, respectively. The uncertainty set of the uncontrollable load ψ_t is $[30, 40]$. Thus, the overall uncertainty set of $\sum_i b_t^i + \psi_t$ is $[58, 75]$, whose upper and lower bounds are shown as the green dotted lines in Fig. 1 and Fig. 2. Each building's VB is given by $\mathcal{B}(2.5, 4.8, \infty, a)$, where we will vary a in our experiment between $a = 0.08$ (low dissipation case, Fig. 1) and $a = 0.5$ (high dissipation case, Fig. 2). We form an aggregate VB with parameters $\mathcal{B}(9.50, 18.24, \infty, a)$, where the dissipation rate a is identical to that of each building. We compare our solution with the following benchmark algorithms. "MPC-DVBC" means MPC with direct-VB control. It assumes the same direct-VB control setting and uses the same aggregate VB (described above) as our EPS algorithm. However, at each time it predicts the future inputs as the mid-points of the uncertainty set, and minimizes the future peak using the predicted inputs. It then only executes the aggregate consumption decision for the current time-slot. "MPC-price" means MPC with price-based control. It aims to use price signals to attain the same aggregate consumption decision as MPC-DVBC. We can formulate a similar optimization problem as (11), except that the decision variables β_i and all constraints related to Theorem 4.1 are removed. A distributed dual-based solution can then be derived similarly to Algorithm 1. Our robustified algorithm will robustify MPC-DVBC into an algorithm with the same CR as the EPS algorithm. Then it uses the price-based control framework in Section 4.2. Each well-behaved building has a payoff function $U_t^i(e_t^i)$ of the form: $p \cdot e_t^i - 0.002(e_t^i - b_t^i)^2$. We choose this form for the desirable property that, when the current electricity price is equal to the nominal price p, each building will consume its baseload b_t^i. We use a nominal price p of 0.12, and the values of P_{high} and P_{low} are 0.1 and 0.2, respectively. For the actual realizations, we experiment with three trajectories: the lower bound trajectory (Fig. 1(a) & 2(a)), the upper bound trajectory (Fig. 1(b) & 2(b)) and the trajectory with a later peak (Fig. 1(c) & 2(c)). In our experiments, we assume that one in four buildings are misbehaving in the sense that they are not responsive to the price signals (i.e., they always stick to their baseload consumption).

Fig. 1 shows the performance comparison for the low dissipation case ($a = 0.08$). In each subfigure, the blue dot displays the actual trajectory, the yellow line represents the decision of MPC-DVBC,

the black line shows the decision of MPC-price, and the pink crosses shows the decision of our robustified algorithm with price-based control. A general trend is that our robustified algorithm attains either the same or a lower peak than MPC-DVBC and MPC-price. Specifically, in Fig. 1(a) (the lower bound trajectory), both versions of MPC would charge at a higher level than our robustified algorithm at the beginning. This is because MPC predicts the future trajectory as the midpoint between the lower and upper bounds of the uncertainty set. In contrast, EPS uses the lower bound to compute the peak estimate, which, after multiplied by CR, is still lower than the decision of MPC. Thus, the robustified algorithm will follow the decision of EPS, which leads to a lower peak overall. Further, we can verify that the higher peak of MPC in the first few slots already leads to a higher CR than the optimal CR. Fig. 1(c) illustrates a different scenario where the peak occurs towards the end. Note that at time-slots 21, our robustified algorithm follows the same decision as that of MPC-DVBC. (The EPS decision would have been higher in this case.) However, MPC-price produces a higher peak. This is because MPC-price loses some flexibility when one of the buildings stick to its baseload regardless of the price incentives. Therefore, MPC-price can no longer discharge the same amount as MPC-DVBC.

Fig. 2 is similar to Fig. 1, but is for the high dissipation case ($a = 0.5$). While the general trends are similar, there are also a few notable differences. First, in Fig. 2(a), not only does the robustifed algorithm attain a lower peak than MPC at the beginning (similar to Fig. 1(a)), it also consumes consistently less at later times. Recall that, as in Fig.1(a), the robustified algorithm would incur lower consumption at the beginning since it computes the peak estimate using the lower bound inputs for the future (in contrast to MPC that uses the midpoint between the upper/lower bounds as future prediction). In Fig. 1(a), the higher consumption level of MPC will soon fully charge the VBs, and thus the subsequent consumption of MPC will be lower. In contrast, in Fig. 2(a), the VBs will keep losing charge due to dissipation, which is the reason why the MPC decisions remain at a higher level. For Fig. 2(b), we can also observe a visible difference between MPC-DVBC and MPC-price. Such difference is much smaller in Fig. 1(b). The reason for this difference is that MPC with DVBC tries to discharge a lot more in Fig. 2(b). Thanks to the high dissipation rate, the SoC will return to a value closer to zero every time-slot, and thus MPC-DVBC can continue to discharge in subsequent time-slots. Since one building mis-behaves, it is no longer possible for MPC-price to discharge the same amount, which leads to the gap not seen in Fig. 1(b). On the other hand, for Fig. 2(c), we no longer observe a difference between MPC-DVBC and MPC-price at the later peak (as in Fig. 1(c)). The reason is that the MPC-DVBC discharges less in Fig. 2(c) than in Fig. 1(c), due to the VB dissipation in previous time-slots. Hence, even with one building mis-behaving, MPC-price can still discharge a similar amount.

Finally, in Fig. 3 we vary the aggregate VB capacity from 3.8 to 17.1, and plot the optimal CR (attained by EPS) and the empirical competitive ratio (ECR) of MPC-DVBC under the lower bound trajectory. It is clear that the empirical CR of MPC is consistently higher than the optimal CR attained by EPS across the whole range of VB capacity. Similar trends (not shown) also hold when we vary other VB parameters.

6.2 Realistic trace

For simulation with realistic trace, we use the data sets of Elia [1], which provides day-ahead prediction and real-time consumption of demand and renewable generation amount for every 15 minutes. We first aggregate the raw data into hourly consumption and prediction. We then use scaled-down version of the total demand and renewable generation of [1] to generate the baseload of buildings and the uncontrollable load. Specifically, we first scale down the total demand data in Elia by a factor of 1,000. The resulted demand is around 9400 KW. From [14], the demand of a single-family house is around 2.5 KW. Thus, our scaled-down demand roughly corresponds to an area with 3750 single-family houses. Further, we assume that the demand of a (commercial) building is higher and is about 15 times that of a single-family house. Thus, we scale down Elia's demand data by $1000 * 3750/15 = 250K$, to obtain the baseload of a building. We then consider 20 buildings that participate in our demand response program. This roughly corresponds to about 8% of the load participating. We also scale down Elia's renewable data by 1000, to simulate an area with the same level of renewable penetration as Elia, which is at about 20%. We then subtract the 20 building's load and the renewable generation from the area's total load, which becomes the uncontrollable load. With this setup, the resulted total baseload of controllable buildings is around 700KW, and the uncontrollable load is around 6000KW. The choices of payoff function $U_t^i(e_t^i)$, nominal price p, and P_{high} and P_{low} are the same as Section 6.1.

Note that the uncertainty set Y for EPS (or robustified algorithm) requires lower/upper bounds of B_t and ψ_t for each time-slot. However, the day-ahead prediction from Elia [1] only contains one value. In order to obtain a lower and an upper bound of prediction, we compare the difference between day-ahead predicted value and its real value over a period of time (e.g., a year). We can then compute the lower and upper bounds of the prediction error (we use a confidence interval of 99%). We then add these prediction error bounds to the day-ahead prediction of Elia, to obtain the uncertainty set Y.

To obtain the VB parameters, we apply the method of [13] to a single-family house, and estimate the capacity and the discharging limit as 4.5 KWh and 3.3 KW per house. Since we assume that a building corresponds to 15 single-family houses, we take the VB capacity of a building as 64KWh and its discharging limit as 50 KW. Consistent with our model, we assume that the charging limit is ∞. We first simulate a scenario with dissipation factor $a = 0.5$ (i.e., a poorly-insulated building with high dissipation). Finally, when we aggregate the 20 VBs together, we use an aggregate VB of parameter $\mathcal{B} = (1216, 950, \infty, 0.5)$.

Fig. 4 shows the result of applying the robustified algorithm to a "difficult" day (April 6th, 2020). This is similar to the synthetic trace Fig. 2(a) in the sense that the actual realization is consistently lower than the prediction most of the time. Therefore, we expect that MPC will incur higher consumption than EPS (due to its use of the higher predicted values for the future), which will lead to a higher empirical competitive ratio as in Fig. 2(a). Interestingly, the existence of misbehaving buildings mitigates this effect a little bit. Indeed, we assume that 25% of buildings are misbehaving (i.e., sticking to their baseload). We can observe that the consumption of MPC-price is in fact lower than MPC-DVBC (because some

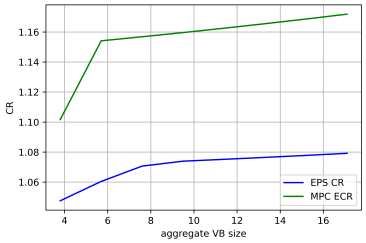

Figure 3: Comparison of CR with different VB capacity ($a = 0.08$)

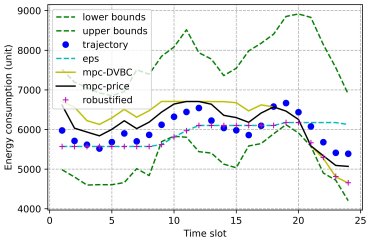

Figure 4: Difficult Trace: 97th day of the year.

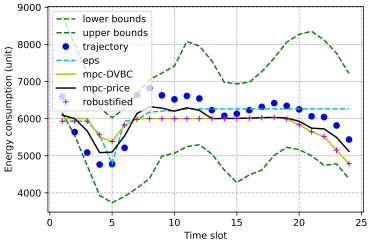

Figure 5: Difficult Trace: 144th day of the year.

buildings do not increase their consumptions as dictated by MPC-DVBC). Nonetheless, for both version of MPC, the optimal CR is still violated for over half of the time slots. Furthermore, the peak of our robustified algorithm is much lower. This figure can be compared to Fig. 2(a), where MPC also incurs much higher consumption than the robustified algorithm due to the use of a higher prediction.

Fig. 5 demonstrates another difficult trajectory for MPC-price for a different day (May 23, 2020). This is similar to the synthetic trace Fig. 2(c) in the sense that, while the realized input at the beginning of the time-horizon is lower than the prediction, the input around time-slot 7 to 10 increases to values higher than the prediction. As in Fig. 2(c), MPC-price will have difficulty lowering the peak when the high input occurs, because some of the buildings may not respond to price signals. Specifically, we assume that 50% of the total buildings are misbehaving and sticking to their baseload. We observe that at the 8th time slot, MPC-price is having a hard time converging to the decision of MPC-DVBC. This is due to both the discharging limit imposed on aggregate VB and 50% of the buildings misbehaving. After the well-behaved buildings are nearly fully discharged, it becomes difficult for MPC-price to attain the same decision as MPC-DVBC at the 8th time-slot. It is also interesting to note that for both figures, robustification plays a huge role in improving the energy consumption at every time slot. It intelligently switches between MPC-DVBC and EPS, so that not only the optimal CR is attained, the actual consumption level is also low in most time-slots.

One impression that readers may get from Fig. 4 and Fig. 5 is that the change of peak-demand of the robustified algorithm is not very large. This is mainly because our controllable load is only about 8% of the total load. Therefore, most of the load is uncontrollable, making the peak-demand high. To more easily appreciate the peak-demand reduction, we use an alternative metric that compares the peak-demand reduction (i.e., the difference between the original peak demand without invoking flexibility and the new peak demand after invoking flexibility) of each algorithm with the peak-demand reduction of the offline optimal decision. This metric is then less sensitive to the amount of uncontrollable load. The results are reported in Table 2. As we can see from the second row, for day 97, our robustified algorithm can achieve 62.44% of the offline-optimal peak reduction. In contrast, the peak-demand reductions of MPC-DVBC and MPC-price are both negative, implying that their peak is even higher than the original peak without flexibility. This result thus clearly demonstrates the inefficiency of MPC in dealing with future uncertainty. Similarly, for day 144, while our robustified algorithm achieves the same peak-demand reduction as MPC-DVBC (which is around 91.24% of the offline optimal), MPC-price only attains 57.89% of the peak-demand reduction of the offline optimal, which again illustrates the advantage of the flexibility contract and reserve prices in dealing with buildings that may be non-responsive. Finally, we also simulate the case with $a = 0.08$ (i.e., a well-insulated building). The results are reported in the 3rd and 4th rows of Table 2, which show similar advantage of our proposed solution over MPC-price.

Day	Offline	MPC-DVBC	MPC-price	Robustified
97 (a=0.5)	788.57	-40.09 (-0.05%)	-38.91 (-0.05%)	492.35 (62.44%)
144 (a=0.5)	863.76	788.09 (91.24%)	500 (57.89%)	788.09 (91.24%)
97 (a=0.08)	583.19	-119.26 (-20.44%)	-119.26 (-20.44%)	67.10 (11.49%)
144 (a=0.08)	737.20	436.79 (59.25%)	260.33 (35.31%)	454.80(61.69%)

Table 2: Peak-demand reduction of different algorithms

7 CONCLUSION AND FUTURE WORK

In this paper, we propose a price-based control framework for demand response of buildings. Our main contribution is to provide a distributed online algorithm that can attain competitive performance guarantees in terms of reducing the system peak demand under future uncertainty. Further, with a robustification procedure, our solution can not only attain the optimal CR, but also do well for average-case inputs.

A highly desirable feature of our proposed solution is that most of the complexity occurs at the utility side, e.g., to compute the right price signals and the desirable aggregate consumption. The buildings only need to respond to the price signals to maximize their own payoff, which is typical in most price-based demand response work [7]. With the advance in smart buildings and building automation, mechanisms are already developed for buildings to predict [26] and control [11] their load, which can then be readily used in our proposed framework. For future work, an interesting question is how to incorporate the charging power limits m_+ of the VBs (which we assume to be infinity in this paper). Further, we also plan to conduct larger-scale simulation studies to verify the scalability of our algorithm.

8 ACKNOWLEDGMENT

This work has been partially supported by U.S. Department of Energy, Office of Electricity, with grant DE-OE0000921 and under contract DE-AC05-00OR22725, and by NSF through grant ECCS-2129631.

REFERENCES

[1] 2020. Grid data overview. https://www.elia.be/en/grid-data

[2] Abdul Afram and Farrokh Janabi-Sharifi. 2014. Theory and applications of HVAC control systems–A review of model predictive control (MPC). *Building and Environment* 72 (2014), 343–355.

[3] Yuvraj Agarwal, Bharathan Balaji, Seemanta Dutta, Rajesh K. Gupta, and Thomas Weng. 2011. Duty-cycling buildings aggressively: The next frontier in HVAC control. In *Proceedings of the 10th ACM/IEEE International Conference on Information Processing in Sensor Networks*. 246–257.

[4] M.H. Albadi and E.F. El-Saadany. 2008. A summary of demand response in electricity markets. *Electric Power Systems Research* 78, 11 (2008), 1989–1996. https://doi.org/10.1016/j.epsr.2008.04.002

[5] M. H. Albadi and E. F. El-Saadany. 2007. Demand Response in Electricity Markets: An Overview. In *2007 IEEE Power Engineering Society General Meeting*. 1–5. https://doi.org/10.1109/PES.2007.385728

[6] Kadir Amasyali, Mohammed Olama, and Aniruddha Perumalla. 2020. A Machine Learning-based Approach to Predict the Aggregate Flexibility of HVAC Systems. In *2020 IEEE Power Energy Society Innovative Smart Grid Technologies Conference (ISGT)*. 1–5. https://doi.org/10.1109/ISGT45199.2020.9087695

[7] Gianni Bianchini, Marco Casini, Antonio Vicino, and Donato Zarrilli. 2016. Demand-response in building heating systems: A Model Predictive Control approach. *Applied Energy* 168 (2016), 159–170.

[8] Stephen Boyd and Lieven Vandenberghe. 2004. *Convex optimization*. Cambridge University Press.

[9] Peter Cappers, Charles Goldman, and David Kathan. 2010. Demand response in U.S. electricity markets: Empirical evidence. *Energy* 35, 4 (2010), 1526–1535. https://doi.org/10.1016/j.energy.2009.06.029

[10] Chen Chen, Jianhui Wang, and Shalinee Kishore. 2014. A Distributed Direct Load Control Approach for Large-Scale Residential Demand Response. *IEEE Transactions on Power Systems* 29, 5 (2014), 2219–2228. https://doi.org/10.1109/TPWRS.2014.2307474

[11] Han Chen, Paul Chou, Sastry Duri, Hui Lei, and Johnathan Reason. 2009. The design and implementation of a smart building control system. In *2009 IEEE International Conference on e-Business Engineering*. IEEE, 255–262.

[12] Peter Cramton, Axel Ockenfels, and Steven Stoft. 2013. Capacity market fundamentals. *Economics of Energy & Environmental Policy* 2, 2 (2013), 27–46.

[13] Jin Dong, Michael Starke, Borui Cui, Jeffrey Munk, Evgeniya Tsybina, Christopher Winstead, Yaosuo Sonny Xue, Mohammed Olama, and Teja Kuruganti. 2020. Battery Equivalent Model for Residential HVAC. In *2020 IEEE Power Energy Society General Meeting (PESGM)*. 1–5. https://doi.org/10.1109/PESGM41954.2020.9281418

[14] Dheeru Dua and Casey Graff. 2017. UCI Machine Learning Repository. http://archive.ics.uci.edu/ml

[15] Javad Fattahi, Mikhak Samadi, Melike Erol-Kantarci, and Henry Schriemer. 2020. Transactive Demand Response Operation at the Grid Edge using the IEEE 2030.5 Standard. *Engineering* 6, 7 (2020), 801–811. https://doi.org/10.1016/j.eng.2020.06.005

[16] Gohar Gholamibozanjani and Mohammed Farid. 2020. Peak load shifting using a price-based control in PCM-enhanced buildings. *Solar Energy* 211 (2020), 661–673. https://doi.org/10.1016/j.solener.2020.09.016

[17] He Hao, Borhan M. Sanandaji, Kameshwar Poolla, and Tyrone L. Vincent. 2013. A generalized battery model of a collection of Thermostatically Controlled Loads for providing ancillary service. In *2013 51st Annual Allerton Conference on Communication, Control, and Computing (Allerton)*. 551–558. https://doi.org/10.1109/Allerton.2013.6736573

[18] He Hao, Borhan M. Sanandaji, Kameshwar Poolla, and Tyrone L. Vincent. 2015. Aggregate Flexibility of Thermostatically Controlled Loads. *IEEE Transactions on Power Systems* 30, 1 (2015), 189–198. https://doi.org/10.1109/TPWRS.2014.2328865

[19] Justin T. Hughes, Alejandro D. Domínguez-García, and Kameshwar Poolla. 2015. Virtual Battery Models for Load Flexibility from Commercial Buildings. In *2015 48th Hawaii International Conference on System Sciences*. 2627–2635. https://doi.org/10.1109/HICSS.2015.316

[20] Nick Jenkins, Kithsiri Liyanage, Jianzhong Wu, and Akihiko Yokoyama. 2012. *Smart Grid*. Wiley.

[21] Yi Liu, Liye Xiao, Guodong Yao, and Siqi Bu. 2019. Pricing-based demand response for a smart home with various types of household appliances considering customer satisfaction. *IEEE access* 7 (2019), 86463–86472.

[22] Mehdi Maasoumy, Catherine Rosenberg, Alberto Sangiovanni-Vincentelli, and Duncan S Callaway. 2014. Model predictive control approach to online computation of demand-side flexibility of commercial buildings hvac systems for supply following. In *2014 American Control Conference*. IEEE, 1082–1089.

[23] Jacob Mattingley, Yang Wang, and Stephen Boyd. 2011. Receding horizon control. *IEEE Control Systems Magazine* 31, 3 (2011), 52–65.

[24] Yanfang Mo, Qiulin Lin, Minghua Chen, and Si-Zhao Joe Qin. 2021. Optimal Online Algorithms for Peak-Demand Reduction Maximization with Energy Storage. In *Proceedings of the Twelfth ACM International Conference on Future Energy Systems* (Virtual Event, Italy) *(e-Energy '21)*. Association for Computing Machinery, New York, NY, USA, 73–83. https://doi.org/10.1145/3447555.3464857

[25] Ioannis Paschalidis, Binbin Li, and Michael Caramanis. 2011. A market-based mechanism for providing demand-side regulation service reserves. 21–26. https://doi.org/10.1109/CDC.2011.6160541

[26] Muhammad Qamar Raza and Abbas Khosravi. 2015. A review on artificial intelligence based load demand forecasting techniques for smart grid and buildings. *Renewable and Sustainable Energy Reviews* 50 (2015), 1352–1372. https://doi.org/10.1016/j.rser.2015.04.065

[27] Gaurav Sharma, Le Xie, and P. R. Kumar. 2013. Large population optimal demand response for thermostatically controlled inertial loads. In *2013 IEEE International Conference on Smart Grid Communications (SmartGridComm)*. 259–264. https://doi.org/10.1109/SmartGridComm.2013.6687967

[28] Marek Toman, Radoslav Cipin, Dalibor Cervinka, Pavel Vorel, and Petr Prochazka. 2016. Li-ion battery charging efficiency. *ECS Transactions* 74, 1 (2016), 37.

[29] Vahid Vakiloroaya, Bijan Samali, Ahmad Fakhar, and Kambiz Pishghadam. 2014. A review of different strategies for HVAC energy saving. *Energy conversion and management* 77 (2014), 738–754.

[30] Wikipedia contributors. 2021. Young's convolution inequality — Wikipedia, The Free Encyclopedia. https://en.wikipedia.org/w/index.php?title=Young%27s_convolution_inequality&oldid=1026506182. [Online; accessed 9-February-2022].

[31] Xiaomin Xi and Ramteen Sioshansi. 2014. Using Price-Based Signals to Control Plug-in Electric Vehicle Fleet Charging. *IEEE Transactions on Smart Grid* 5, 3 (2014), 1451–1464. https://doi.org/10.1109/TSG.2014.2301931

[32] Xiaojing Xu, Chien fei Chen, Xiaojuan Zhu, and Qinran Hu. 2018. Promoting acceptance of direct load control programs in the United States: Financial incentive versus control option. *Energy* 147 (2018), 1278–1287. https://doi.org/10.1016/j.energy.2018.01.028

[33] A. Zakaria, Firas B. Ismail, M.S. Hossain Lipu, and M.A. Hannan. 2020. Uncertainty models for stochastic optimization in renewable energy applications. *Renewable Energy* 145 (2020), 1543–1571. https://doi.org/10.1016/j.renene.2019.07.081

[34] Shizhen Zhao, Xiaojun Lin, and Minghua Chen. 2017. Robust Online Algorithms for Peak-Minimizing EV Charging Under Multistage Uncertainty. *IEEE Trans. Automat. Control* 62, 11 (2017), 5739–5754. https://doi.org/10.1109/TAC.2017.2699290

A THE CORRECTNESS OF ABS AND CONVERSION INTO ABS

In Section 5, we introduce ABS algorithm, whose detailed specification is given in Algorithm 2.

Algorithm 2: A class of ABS Algorithms

Input : Time-slot t, the baseline and uncontrollable load at t (i.e., O_t), and Z_t that has been revealed

Output : Aggregate consumption decision E_t

1 Choose E'_t as any value between $\eta^* E_t^{\text{pe}}(Z_t)$ and $\max\{\max_{t_1 \geq t}(R^*_{\eta^*_Y}(Z_t, t_1)) + O_t\}, O_t - m_-\}$;

2 If $E'_t < O_t$, we would discharge $E'_t - O_t$ amount and $E_t = E'_t$. If $E'_t > O_t$ then the difference $E'_t - O_t$ would be charged to aggregate VB. However, if as a result the aggregate VB is overcharged, we will further reduce E'_t to $E_t = C - (1-a)x_{t-1}$ such that the VB is exactly full.

For such an ABS algorithm to be meaningful, however, we need to ensure that the upper bound $\eta^* E_t^{\text{pe}}(Z_t)$ is always no smaller than the lower bound $\max\{\max_{t_1 \geq t}(R^*_{\eta^*_Y}(Z_t, t_1)) + O_t, O_t - m_-\}$. This is ensured by the following lemma.

Lemma A.1. *Given $Z \in Z_Y$, for any algorithm π in ABS, at each time slot t, we must have:*

$$\max_{t_1 \geq t}(R^*_{\eta^*_Y}(Z_t, t_1)) + O_t \leq \eta^*_Y E_t^{\text{pe}}(Z_t), \tag{17}$$

$$O_t - m_- \leq \eta^*_Y E_t^{\text{pe}}(Z_t). \tag{18}$$

Proof. Recall from (15) and (16) that $\max_{t_1 \geq t}(R^*_{\eta^*_Y}(Z_t, t_1))$ corresponds to the smallest value of $E_t(Z_t, \pi) - O_t$ that satisfies inequalities (14) for all possible t_1's and all possible future realizations. In order to show (17), or equivalently, $\eta^*_Y E^{\text{pe}}_t(Z_t) - O_t \geq \max(R^*_{\eta^*_Y}(Z_t, t_1))$, it is sufficient to show that $\eta^*_Y E^{\text{pe}}_t(Z_t) - O_t$ is no smaller than the RHS of (14) for all $t_1 \geq t$ and all possible future realizations. In other words,

$$(1-a)^{t_1-t}(\eta^*_Y E^{\text{pe}}_t(Z_t) - O_t) \geq \sum_{s=t+1}^{t_1}(1-a)^{t_1-s}O_s - C$$
$$-(1-a)^{t_1+1-t}x_t - \eta^*_Y \sum_{s=t+1}^{t_1}(1-a)^{t_1-s}E^{\text{pe}}_s(Z_s).$$

Equivalently,

$$\eta^*_Y \sum_{s=t}^{t_1}(1-a)^{t_1-s}E^{\text{pe}}_s(Z_s) \geq \sum_{s=t}^{t_1}(1-a)^{t_1-s}O_s - C - (1-a)^{t_1+1-t}x_t. \tag{19}$$

We prove that (19) holds by induction on t. When $t = 1$, using $x_1 = 0$ (from (2)), we need to show:

$$\eta^*_Y \geq \frac{\sum_{s=1}^{t_1}(1-a)^{t_1-s}O_s - C}{\sum_{s=1}^{t_1}(1-a)^{t_1-s}E^{\text{pe}}_s(Z_s)}.$$

This follows immediately from the first expression in (10) and the definition of η^*_Y in Theorem 3.2.

Assume that inequality (19) holds for a given t and $t_1 \geq t$. By Lemma A.2 below, we have $E_t \geq \max_{t_1 \geq t}(R^*_{\eta^*_Y}(Z_t, t_1)) + O_t$ after choosing the value of E_t in Step 2 of Algorithm 2. (Note that Lemma A.2 can be proved independently of Lemma A.1. Hence, we can use the result of Lemma A.2 here.) Next we will show that (19) holds for $t+1$ and all $t_1 \geq t+1$. We prove by contradiction.

Assume in the contrary that there exists $\tilde{t}_1 \geq t+1$ and $\tilde{O}_s$ such that:

$$\eta^*_Y \sum_{s=t+1}^{\tilde{t}_1}(1-a)^{\tilde{t}_1-s}E^{\text{pe}}_s(\tilde{Z}_s) < \sum_{s=t+1}^{\tilde{t}_1}(1-a)^{\tilde{t}_1-s}\tilde{O}_s - C - (1-a)^{\tilde{t}_1-t}x_{t+1}.$$

Then, after reorganizing the terms, we have:

$$0 < \sum_{s=t+1}^{\tilde{t}_1}(1-a)^{\tilde{t}_1-s}\tilde{O}_s - C - (1-a)^{\tilde{t}_1-t}x_{t+1}$$
$$- \eta^*_Y \sum_{s=t+1}^{\tilde{t}_1}(1-a)^{\tilde{t}_1-s}E^{\text{pe}}_s(\tilde{Z}_s). \tag{20}$$

Note that from (2), $-(E_t - \tilde{O}_t) = (1-a)x_t - x_{t+1}$. Multiplying both sides by $(1-a)^{\tilde{t}_1-t}$, we have:

$$0 = (1-a)^{\tilde{t}_1+1-t}x_t - (1-a)^{\tilde{t}_1-t}x_{t+1} - (1-a)^{\tilde{t}_1-t}\tilde{O}_t + (1-a)^{\tilde{t}_1-t}E_t. \tag{21}$$

Subtracting the RHS of (21) from the RHS of inequality (20), we have:

$$0 < \sum_{s=t+1}^{\tilde{t}_1}(1-a)^{\tilde{t}_1-s}\tilde{O}_s - C - (1-a)^{\tilde{t}_1-t}x_{t+1}$$
$$- \eta^*_Y \sum_{s=t+1}^{\tilde{t}_1}(1-a)^{\tilde{t}_1-s}E^{\text{pe}}_s(\tilde{Z}_s) - (1-a)^{\tilde{t}_1+1-t}x_t$$
$$+(1-a)^{\tilde{t}_1-t}x_{t+1} + (1-a)^{\tilde{t}_1-t}\tilde{O}_t - (1-a)^{\tilde{t}_1-t}E_t.$$

Note that the third and sixth terms of the RHS cancel out. We then have:

$$0 < (1-a)^{\tilde{t}_1-t}\max_{t_1 \geq t}(R^*_{\eta^*_Y}(\tilde{Z}_t, \tilde{t}_1)) + (1-a)^{\tilde{t}_1-t}\tilde{O}_t - (1-a)^{\tilde{t}_1-t}E_t.$$

The last inequality holds based on the definition of the optimization problem (15). The above derivation implies that $E_t < O_t + \max_{\tilde{t}_1 \geq t}(R^*_{\eta^*_Y}(\tilde{Z}_t, \tilde{t}_1))$, which contradicts to our choice of E_t. Hence, (19) holds for $t+1$ and all $t_1 \geq t+1$. By induction, inequality (19) holds for all t's and $t_1 \geq t$.

Regarding inequality (18), we have, from the definition of η^*_Y (the second expression in (10)):

$$\eta^*_Y \geq \frac{O_t - m_-}{E^{\text{pe}}_t(Z_t)}. \tag{22}$$

Then, we have $\eta^*_Y E^{\text{pe}}_t(Z_t) \geq O_t - m_-$. □

Lemma A.1 implies it is always feasible to choose E'_t in Step 1 of Algorithm 2. The following Lemma A.2 further shows that, even after the potential reduction from E'_t to E_t in step 2 of Algorithm 2, the value of E_t must always be larger than or equal to $\max\{\max_{t_1 \geq t}(R^*_{\eta^*_Y}(Z_t, t_1)) + O_t, O_t - m_-\}$. Note that Lemma A.2 is proved independently of Lemma A.1 and hence its result can also be used in the proof Lemma A.1.

Lemma A.2. *For any given t, if E'_t exists in step 1 of ABS, (i.e., the lower bounds is not greater than the upper bound), we must have, after step 2 of ABS*

$$\max_{t_1 \geq t}(R^*_{\eta^*_Y}(Z_t, t_1)) + O_t \leq E_t \leq \eta^*_Y E^{\text{pe}}_t(Z_t),$$
$$O_t - m_- \leq E_t.$$

where E_t is the energy consumption after potential reduction.

Proof. First, it is easy to see that, in the first inequality of the statement of Lemma A.1, $E_t \leq \eta^*_Y E^{\text{pe}}_t(Z_t)$ must be true since we get E_t from E'_t by potentially reducing energy consumption and E'_t is no more than $\eta^*_Y E^{\text{pe}}_t(Z_t)$.

To see why $E_t \geq \max_{t_1 \geq t}(R^*_{\eta^*_Y}(Z_t, t_1)) + O_t$, we have two scenarios to consider. One is that a reduction does not happen at time t, then the result follows trivially. The other scenario assumes that a reduction does happen at time t. In other words, the overcharging happens at time t. Then, from Algorithm 2 we have that the charging amount $E_t - O_t$ must make the VB full. Recall that $\max_{t_1 \geq t}(R^*_{\eta^*_Y}(Z_t, t_1)) + O_t$ is the lower bound for E_t to ensure that, if all future consumption is equal to $\eta^*_Y E^{\text{pe}}_{t_1}(Z_{t_1})$, the VB is never over-discharged. However, now that VB is already charged to full by E_t, there should not be any concern for VB to be over-discharged later. Thus, intuitively we should have $E_t \geq \max_{t_1 \geq t}(R^*_{\eta^*_Y}(Z_t, t_1)) + O_t$. For a rigorous proof, using battery evolution Equation (2), we have $C = (1-a)x_t + E_t - O_t$. Rearranging the terms, we have $E_t = -(1-a)x_t + O_t + C$. Furthermore, from inequality (9) and the definition of η^* in

Theorem 3.2, we have that, for all t_1 and t_2, and for all possible future realizations:

$$\eta^* \geq \frac{\sum_{t=t_1}^{t_2}(1-a)^{t_2-t}O_t - C - C(1-a)^{t_2-t_1+1}}{\sum_{t=t_1}^{t_2}(1-a)^{t_2-t}E_t^{\text{pe}}(Z_t)}.$$

Equivalently, (i.e., multiplying the denominator on both sides):

$$\eta^*\sum_{t=t_1}^{t_2}(1-a)^{t_2-t}E_t^{\text{pe}}(Z_t) \geq \sum_{t=t_1}^{t_2}(1-a)^{t_2-t}O_t - C - C(1-a)^{t_2-t_1+1}.$$

If we replace t_1 by $t+1$, t_2 by t_1, and rearrange terms, we have:

$$C(1-a)^{t_1-t} \geq \sum_{s=t+1}^{t_1}(1-a)^{t_1-s}O_s - C - \eta^*\sum_{s=t+1}^{t_1}(1-a)^{t_1-s}E_s^{\text{pe}}(Z_s).$$

Add $-(1-a)^{t_1-t+1}x_t$ on both sides, then divide both sides by $(1-a)^{t_1-t}$. Finally add O_t on both sides. We then have (Note that this holds for all $t_1 \geq t$, and all possible future realizations):

$$\begin{aligned} -(1-a)x_t + O_t + C \geq{}& \frac{\sum_{s=t+1}^{t_1}(1-a)^{t_1-s}O_s - C}{(1-a)^{t_1-t}} \\ &+ \frac{-(1-a)^{t_1-t+1}x_t - \eta^*\sum_{s=t+1}^{t_1}(1-a)^{t_1-s}E_s^{\text{pe}}(Z_s)}{(1-a)^{t_1-t}} + O_t. \end{aligned} \quad (23)$$

Note that the LHS of (23) is E_t, and the first and second terms of the RHS of (23) are the same as the RHS of (14). Since the above inequality holds for all $t_1 \geq t$ and all possible future realizations, we have:

$$\begin{aligned} E_t &\geq \max_{t_1 \geq t}\left(\max_{Z' \in Z_Y : Z'_t = Z_t} \text{RHS of (23)}\right) \\ &= \max_{t_1 \geq t}(R^*_{\eta^*_Y}(Z_t, t_1)) + O_t, \end{aligned}$$

where the last equality is based on (15) and (16).

Next, we need to see why the second inequality of the lemma holds. Again, there are two scenarios to consider. One is that a reduction does not happen at t, then the result follows trivially. The other assumes that the reduction does happen at time t. In other words, overcharge occurs at time t. Thus, we must have $E_t^{'} - O_t \geq 0$. To avoid overcharge, we do not need to reduce $E_t^{'}$ to below O_t. That is, $E_t \geq O_t$. Hence, $E_t \geq O_t - m_-$. □

Combining Lemmas A.1 and A.2, we can conclude that the ABS algorithm is always well-defined. The following lemma shows that all ABS algorithms are indeed optimal.

Lemma A.3. *Any algorithm π in the class ABS is feasible and achieves the optimal competitive ratio of η^*_Y.*

Proof. This proof is straightforward. Since $E_t \leq \eta^* E_t^{\text{pe}}(Z_t)$, and the future offline peak is at least $E_t^{\text{pe}}(Z_t)$, the peak of algorithm π will never exceed η^*_Y times the offline optimal peak. Thus, the algorithm π is η^*_Y-competitive. It only remains to check that it always respects the limit of the aggregate VB. From step 2 of Algorithm 1, the VB is never over-charged. To show that the VB is never over-discharged, let $t = t_1$ in the statement of Lemma A.2, we have $E_t(Z_t, \pi) \geq R^*_{\eta^*_Y}(Z_t, t) + O_t$. Consider the definition of $R^*_{\eta^*_Y}(Z_t, t)$ in (14) and (15) again. By replacing t_1 with t in the RHS of (14) and using the convention that $\sum_{s=t+1}^{t} = 0$, we have $R^*_{\eta^*_Y}(Z_t, t) \geq -(1-a)x_t - C$. We must then have $E_t(Z_t, \pi) \geq O_t - C - (1-a)x_t$. That is, $(E_t(Z_t, \pi) - O_t) + (1-a)x_t \geq -C$. In other words, the VB would never be over-discharged. Finally, Lemma A.2 also ensures that the discharging power limit m_- is met. The result of the lemma then follows. □

A.1 Robustified algorithm

To find an online algorithm in ABS that also has good average performance, our strategy is to take any algorithm with reasonable average-case performance, and convert it into one in the class ABS.

Algorithm 3 is presented to show the procedure of *algorithm-robustification*. Specifically, line 2 calculates the lower bound. Line 3 and 4 adjust the upper bound if it would otherwise overcharge the battery. Line 6 states that , if $E_t(Z_t, \pi_0)$ is between the upper and lower bound, then we use the decision of the original algorithm π_0. Otherwise, we "robustify" the decision by setting the decision to one of the bounds, such that the resulting robustified algorithm belongs to ABS. Finally, note that such a robustified decision can again be used in Section 4 to perform price-based control. As a result, our price-based control will also attain both the optimal competitive ratio and good average-case performance. In our numerical results, we will use MPC with direct-VB control as the algorithm π_0 to produce the robustified algorithm. Please refer to Section 6 for details.

Algorithm 3: Algorithm Robustification Procedure

Input : A realization $Z \in Z_Y$, the optimal competitive ratio η^*_Y and any online algorithm π_0

Output : An optimal online algorithm π_{robust} and its schedule $E_t(Z_t, \pi_{\text{robust}})$

1 **for** *t=1:T* **do**
2 Compute $\alpha = \max\{\max_{t_1 \geq t}(R^*_{\eta^*_Y}(Z_t, t_1)) + O_t\}, O_t - m_-\}$;
3 **if** $(1-a)x_t - E_t(Z_t, \pi_0) + O_t > C$ **then** $\beta = (1-a)x_t + C + O_t$;
4 **else** $\beta = \eta^*_Y E_t^{\text{pe}}(Z_t)$;
5 Set $E_t(Z_t, \pi_{\text{robust}}) = \max\{\min\{E_t(Z_t, \pi_0), \beta\}, \alpha\}$
6 **end**

B PROOF OF LEMMA 3.1

Proof. First, we show that two inequalities are necessary. We can apply battery evolution equation $x_{t+1} - x_t = -ax_t + u_t$ recursively, assuming the SoC at time 0 is 0. And we have $x_{t+1} = \sum_{s=1}^{t}(1-a)^{t-s}u_s$. So it must be between $-C$ and C. Reorganizing the term, we have inequality (4). For (5), suppose there is some $\tilde{t}$ such that $b_{\tilde{t}} + \psi_{\tilde{t}} - m_- \geq E_{\tilde{t}}$. That means the discharging amount must be greater than m_-, which contradicts our assumption.

Second, we show that two inequalities are sufficient. Suppose that there is a time $\tilde{t_2}$ that makes battery overcharge. However, the inequality (4) applied to $\tilde{t_2}$ ensures that it would not overcharge. Similar proof applies to over discharging behavior. For the discharging limit, suppose there is some time $\tilde{t}$ that makes battery discharge faster than m_-. However, the inequality (5) would ensure that behavior never happens. So the two inequalities are sufficient. □

C PROOF OF THEOREM 3.3

Proof. The first part is easy to prove as follows. Note that from definition, we have $E_t^{\text{pe}}(Z_t) = \inf_{Z' \in Z_Y : Z'_t = Z_t} E^*_{\text{off}}(Z)$. Thus, for all $Z \in Z_Y$, we must have $E_t^{\text{pe}}(Z_t) \le E^*_{\text{off}}(Z)$. Since $E_t \le \eta_Y^* E_t^{\text{pe}}(Z_t)$, we must have $E_t \le \eta_Y^* E^*_{\text{off}}(Z)$.

Now we focus on the second part. From the definition of η_Y^* in Theorem 3.2, the following three inequalities must hold:

$$\begin{aligned}
&\forall 1 < t_1 \le t_2 \le T,\\
&\eta_Y^* \ge \sup_{Z \in Z_Y} \frac{\sum_{t=t_1}^{t_2}(1-a)^{t_2-t}(B_t+\psi_t) - C - C(1-a)^{t_2-t_1+1}}{\sum_{t=t_1}^{t_2}(1-a)^{t_2-t}E_t^{\text{pe}}(Z_t)},\\
&\forall t_2 \le T,\\
&\eta_Y^* \ge \sup_{Z \in Z_Y} \frac{\sum_{t=1}^{t_2}(1-a)^{t_2-t}(B_t+\psi_t) - C}{\sum_{t=t_1}^{t_2}(1-a)^{t_2-t}E_t^{\text{pe}}(Z_t)},\\
&\eta_Y^* \ge \sup_{Z \in Z_Y} \frac{(b_{t_2}+\psi_{t_2}) - m_-}{E_{t_2}^{\text{pe}}(Z_t)}. \qquad (24)
\end{aligned}$$

Given any realization Z, let $E'_t = \eta_Y^* E_t^{\text{pe}}(Z_t)$ for all t. Recall that the decision E_t of EPS may be lower than E'_t, only if E'_t will overcharge the aggregate VB. For E'_t, we have, from (24),

$$\begin{aligned}
&\forall t_2 \le T, \sum_{t=1}^{t_2}(1-a)^{t_2-t}(B_t+\psi_t) - C \le \sum_{t=1}^{t_2}(1-a)^{t_2-t}E'_t,\\
&\forall t, B_t+\psi_t - m_- \le E'_t,\\
&\forall 1 < t_1 \le t_2 \le T,\\
&\quad \sum_{t=t_1}^{t_2}(1-a)^{t_2-t}(B_t+\psi_t) - C - C(1-a)^{t_2-t_1+1}\\
&\qquad \le \sum_{t=t_1}^{t_2}(1-a)^{t_2-t}E'_t. \qquad (25)
\end{aligned}$$

Now we prove that using E_t, the SoC is always between $-C$ and C, and the battery discharge no faster than m_-.

Since E_t reduces from E'_t whenever overcharge occurs, it immediately implies that SoC $\le C$ at all time. We next show that, at any time t_2, the SoC under the sequence of decisions E_t is always no smaller than $-C$ (i.e., no overdischarging happens). Note that this statement is trivially true if E_{t_2} has to be decreased from E'_{t_2}, because then the SoC at time t_2 should be C. We then consider the scenario where $E_{t_2} = E'_{t_2}$. We divide into two cases.

Case 1: There exists a time t before t_2 that the EPS algorithm reduces E'_t to E_t. In this case, let γ be the previous time slot closest to t_2 that the algorithm reduces E'_t to E_t. It implies that the battery is fully charged at γ, i.e., $x_{\gamma+1} = C$ according to our notation in (2). Since $E_t = E'_t$ for all $\gamma < t \le t_2$, we must have from (25):

$$\begin{aligned}
\sum_{t=\gamma+1}^{t_2}(1-a)^{t_2-t}E_t &= \sum_{t=\gamma+1}^{t_2}(1-a)^{t_2-t}E'_t\\
&\ge \sum_{t=\gamma+1}^{t_2}(1-a)^{t_2-t}(B_t+\psi_t) - C - C(1-a)^{t_2-\gamma}. \qquad (26)
\end{aligned}$$

By recursively applying the SOC evolution equation (2) from time $\gamma+1$ to t_2, and using $x_\gamma = C$, we have that the SoC at time t_2 (which is x_{t_2+1} according to our notation) is $(1-a)^{t_2-\gamma}C + \sum_{t=\gamma+1}^{t_2}(1-a)^{t_2-t}(E_t - B_t - \psi_t)$. From the above inequality (26), we then have that the SOC at time t_2 must be greater than or equal to $-C$. In other words, the VB would never be discharged more than its capacity.

Case 2: The EPS algorithm does not need to reduce E'_t to E_t for all $t < t_2$. Since $E_t = E'_t$ for all $t \le t_2$, we must have from (25):

$$\begin{aligned}
\sum_{t=1}^{t_2}(1-a)^{t_2-t}E_t &= \sum_{t=1}^{t_2}(1-a)^{t_2-t}E'_t\\
&\ge \sum_{t=1}^{t_2}(1-a)^{t_2-t}(B_t+\psi_t) - C. \qquad (27)
\end{aligned}$$

By recursively applying the SOC evolution equation (2) from time 1 to t_2, and using $x_1 = 0$, we have that the SoC at time t_2 (which is x_{t_2+1} according to our notation) is $\sum_{t=1}^{t_2}(1-a)^{t_2-t}(E_t - B_t - \psi_t)$. From the above inequality (27), we then have that the SOC at time t_2 is greater than or equal to $-C$. In this case, the VB would also never be discharged more than its capacity.

Finally, we show that E_t never discharge the aggregate VB faster than m_-. Note that if $E_t = E'_t$, we must have $E_t \ge B_t + \psi_t - m_-$ from (25). On the hand other, if $E_t < E'_t$, it must be because that overcharge occurs at time t under E'_t. Since E_t would still charge the VB to exactly C, we must have $E_t \ge B_t + \psi_t \ge B_t + \psi_t - m_-$. □

D PROOF OF THEOREM 4.1

According to the assumption of Theorem 4.1, at the end of time $t_c - 1$, the state of charge (SoC) of the aggregate VB is x_{t_c-1} and the state of charge of each individual VB is $x^i_{t_c-1}$. Suppose that the charging/discharging signal $u_t = E_t - B_t - \Psi_t$, $t > t_c$ to the aggregate VB respects the limits of the aggregate VB. Further, suppose that, after t_c, we use β_i to dispatch the charging/discharging signal to building i, i.e., $u^i_t = \beta_i u_t$ for $t > t_c$. Our goal is to show that, as long as β_i satisfies the condition in Theorem 4.1, the individual VB's limits must always be respected.

Towards this end, we re-define the time axis so that $n = 0$ starts from $t = t_c$. More precisely, let $\tilde{x}_n = x_{t_c+n}$ and $\tilde{u}_n = u_{t_c+n}$. From the definition of the VB, we have $\tilde{x}_{n+1} - \tilde{x}_n = -a\tilde{x}_n + \tilde{u}_n$ and $\tilde{x}_0 = x_{t_c}$. Since $\tilde{u}_n$ respects the limits of the aggregate VB, we must have,

$$\begin{aligned}
&-m_- \le \tilde{u}_n, \text{and}\\
&|\tilde{x}_n| \le C. \qquad (28)
\end{aligned}$$

Similarly, re-defining time-axis for the individual VB i, we also have:

$$\tilde{x}^i_{n+1} - \tilde{x}^i_n = -a^i\tilde{x}^i_n + \tilde{u}^i_n, \text{ and } \tilde{x}^i_0 = x^i_{t_c}. \qquad (29)$$

We now take the z-transform of (29). Let $\mathcal{X}^i_z$ denote the z-transform of $\tilde{x}^i_n, n = 0, 1, ...$, i.e.,

$$\mathcal{X}^i_z = \sum_{n=0}^{\infty} z^{-n}\tilde{x}^i_n. \qquad (30)$$

Then, the z-transform of $\tilde{x}^i_{n+1}, n = 0, 1, ...$ is given by $z(\mathcal{X}^i_z - \tilde{x}^i_0)$. Similarly, let U^t_z be the z-transform of $\tilde{u}^i_n, n = 0, 1, ...$, we then have from (29):

$$z\mathcal{X}^i_z - zx^i_{t_c} = (1-a^i)\mathcal{X}^i_z + \mathcal{U}^i_z.$$

Reorganizing the above equation, we have:

$$\mathcal{X}_z^i = \frac{z x_{t_c}^i + \mathcal{U}_z^i}{z + a^i - 1}. \tag{31}$$

For the aggregate VB equation $\tilde{x}_{n+1} - \tilde{x}_n = -a\tilde{x}_n + \tilde{u}_n$ (with the initial condition of $x_0 = x_{t_c}$), we can carry out z-transform similarly and get:

$$\mathcal{X}_z = \frac{z x_{t_c} + \mathcal{U}_z}{z + a - 1}. \tag{32}$$

Reorganizing (32), we have: $\mathcal{U}_z = -z x_{t_c} + (z + a - 1)\mathcal{X}_z$. Now we can use the z-transform of the relation $u_n^i = \beta_i u_n$ (i.e., $\mathcal{U}_z^i = \beta_i \mathcal{U}_z$). Combining it with (31) and (32), we have:

$$\begin{aligned}\mathcal{X}_z^i &= \frac{z x_{t_c}^i + \beta_i \mathcal{U}_z}{z + a^i - 1} \\ &= \frac{z x_{t_c}^i}{z + a^i - 1} + \beta_i \frac{-z x_{t_c}}{z + a^i - 1} + \beta_i \left(1 + \frac{a - a^i}{z + a^i - 1}\right) \mathcal{X}_z. \end{aligned} \tag{33}$$

We now apply the inverse z-transform of (33). Note that the inverse z-transform of $\frac{z}{z+a^i-1}$ is $(1-a^i)^n$, and the inverse z-transform of $\frac{a-a^i}{z+a^i-1}$ is $(a-a^i)(1-a^i)^{n-1}U(n-1)$, where $U(n-1)$ is a step function, i.e., $U(n-1) = 1$ when $n \geq 1$ and 0 otherwise. We then have from (33), for $n = 0, 1...$:

$$\begin{aligned}\tilde{x}_n^i =& x_{t_c}^i (1-a^i)^n - \beta_i x_{t_c} (1-a^i)^n \\ &+ \beta_i (a - a^i)(1-a^i)^{n-1} U(n-1) * \tilde{x}_n + \beta_i \tilde{x}_n, \end{aligned} \tag{34}$$

where $*$ denotes the convolution in time.

We now verify that $\tilde{x}_n^i$ is always within $-C$ and C. Towards this end, for any sequence $\tilde{x}_n, n = 0, 1, ...$, we define $||\tilde{x}_n||_\infty = \max_{n\geq 0} |\tilde{x}_n|$, and $||\tilde{x}_n||_1 = \sum_{n=0}^\infty |\tilde{x}_n|$. Note that since $a^i \leq 1$, we must have $||x_{t_c}^i (1-a^i)^n - \beta_i x_{t_c}(1-a^i)^n||_\infty \leq ||x_{t_c}^i - \beta_i x_{t_c}||_\infty$ for all $n = 0, 1, ...$ Further, using Young's inequality [30], we get:

$$\begin{aligned}&||\beta_i (a-a^i)(1-a^i)^{n-1} U(n-1) * \tilde{x}_n||_\infty \\ \leq& \beta_i ||(a-a^i)(1-a^i)^{n-1} U(n-1)||_1 ||\tilde{x}_n||_\infty \\ \leq& \beta_i \left(\frac{|a-a^i|}{a^i}\right) C, \end{aligned}$$

where the last inequality holds because $\sum_{n=1}^\infty |(1-a^i)^{n-1}| = 1/a^i$ and $||\tilde{x}_n||_\infty \leq C$ from (28).

Substituting these bounds into (34), and using $||a_n + b_n||_\infty \leq ||a_n||_\infty + ||b_n||_\infty$, we then have:

$$||x_n^i||_\infty \leq |x_{t_c}^i - \beta_i x_{t_c}| + \beta_i \left(1 + \frac{|a-a^i|}{a^i}\right) C. \tag{35}$$

We now use the relationship $x_{t_c}^i = (1-a^i) x_{t_c-1}^i + (e_{t_c}^i - b_{t_c}^i)$ and $x_{t_c} = (1-a)x_{t_c-1} + (E_{t_c} - \psi_{t_c} - B_{t_c})$, and substitute them into RHS of (35). We then have for all $n = 0, 1, ...$:

$$\begin{aligned}|x_n^i| \leq \Big| &[(1-a^i) x_{t_c-1}^i + (e_{t_c}^i - b_{t_c}^i)] - \beta_i [(1-a) x_{t_c-1} \\ &+ (E_{t_c} - \psi_{t_c} - B_{t_c})] \Big| + \beta_i \left(1 + \left|\frac{a-a^i}{a}\right|\right) C, i = 1...N, \end{aligned}$$

The first constrain in Theorem 4.1 states that the RHS of the above inequality is no larger than Δ^i. Therefore, the VB $\mathcal{B}^i$'s capacity constraint is always respected.

Next, since the aggregate VB satisfies $u_t \geq -m_-$ and $u_t^i = \beta_i u_t$, we have $u_t^i \geq -\beta_i m_-$. Recall that $\beta_i m_- \leq m_-^i$ from the second constraint of Theorem 4.1. We must then have $u_t^i \geq -m_-^i$. In other words, individual VB's discharge limit is also respected.

Finally, since $\sum_{i=1}^N \beta_i = 1$ and $u_t^i = \beta_i u_t$ for $t > t_c$, we have, for $t > t_c$,

$$\begin{aligned}\sum_{i=1}^N e_t^i &= \sum_{i=1}^N \left[\beta_i (E_t - B_t - \Psi_t) + b_t^i\right] = E_t - B_t - \Psi_t + \sum_{i=1}^N b_t^i \\ &= E_t - \Psi_t. \end{aligned} \tag{36}$$

In other words, the building's consumption adds up to the aggregate consumption decision E_t for all future $t > t_c$. The result of the theorem then follows.

E DERIVATION OF INEQUALITY (6)

We start from inequality (4), which is restated below as two inequalities:

$$\sum_{t=1}^{t_2} (1-a)^{t_2-t} (B_t + \psi_t) - C \leq \sum_{t=1}^{t_2} (1-a)^{t_2-t} E_t \tag{37}$$

$$\sum_{t=1}^{t_2} (1-a)^{t_2-t} E_t \leq \sum_{t=1}^{t_2} (1-a)^{t_2-t} (B_t + \psi_t) + C. \tag{38}$$

In the second inequality (38), replace t_2 with $t_1 - 1$. We then have:

$$\sum_{t=1}^{t_1-1} (1-a)^{t_1-t-1} E_t \leq \sum_{t=1}^{t_1-1} (1-a)^{t_1-t-1} (B_t + \psi_t) + C.$$

Multiplying the above inequality by $-(1-a)^{t_2-t_1+1}$, we have:

$$\begin{aligned}-\sum_{t=1}^{t_1-1} (1-a)^{t_2-t} E_t \geq& \\ &- \sum_{t=1}^{t_1-1} (1-a)^{t_2-t} (B_t + \psi_t) - C(1-a)^{t_2-t_1+1}. \end{aligned}$$

Equivalently, we have:

$$\begin{aligned}-\sum_{t=1}^{t_1-1} (1-a)^{t_2-t} (B_t + \psi_t) - C(1-a)^{t_2-t_1+1} \leq& \\ &- \sum_{t=1}^{t_1-1} (1-a)^{t_2-t} E_t. \end{aligned} \tag{39}$$

Adding the above inequality (39) to the first inequality (37), we obtain:

$$\begin{aligned}&-\sum_{t=1}^{t_1-1} (1-a)^{t_2-t} (B_t + \psi_t) - C(1-a)^{t_2-t_1+1} - C \\ &+ \sum_{t=1}^{t_2} (1-a)^{t_2-t} (B_t + \psi_t) \leq \sum_{t=1}^{t_2} (1-a)^{t_2-t} E_t - \sum_{t=1}^{t_1-1} (1-a)^{t_2-t} E_t. \end{aligned} \tag{40}$$

That is,

$$\sum_{t=t_1}^{t_2} (1-a)^{t_2-t} (B_t + \psi_t) - C - C(1-a)^{t_2-t_1+1} \leq \sum_{t=t_1}^{t_2} (1-a)^{t_2-t} E_t,$$

which is the first inequality in (6). Similarly, we can obtain the second inequality in (6).